

AD _____

CONTRACT NUMBER DAMD17-96-C-6086

TITLE: Thin Film CdZnTe Detector Arrays for Digital Mammography

PRINCIPAL INVESTIGATOR: Rengarajan Sudharsanan, Ph.D.

CONTRACTING ORGANIZATION: Spire Corporation
Bedford, Massachusetts 01730-2396

REPORT DATE: October 1999

TYPE OF REPORT: Annual

PREPARED FOR: U.S. Army Medical Research and Materiel Command
Fort Detrick, Maryland 21702-5012

DISTRIBUTION STATEMENT: Approved for public release;
distribution unlimited

The views, opinions and/or findings contained in this report are those of the author(s) and should not be construed as an official Department of the Army position, policy or decision unless so designated by other documentation.

DTIC QUALITY INSPECTED
20010124 020

REPORT DOCUMENTATION PAGE			Form Approved OMB No. 0704-0188	
Public reporting burden for this collection of information is estimated to average 1 hour per response, including the time for reviewing instructions, searching existing data sources, gathering and maintaining the data needed, and completing and reviewing the collection of information. Send comments regarding this burden estimate or any other aspect of this collection of information, including suggestions for reducing this burden, to Washington Headquarters Services, Directorate for Information Operations and Reports, 1215 Jefferson Davis Highway, Suite 1204, Arlington, VA 22202-4302, and to the Office of Management and Budget, Paperwork Reduction Project (0704-0188), Washington, DC 20503.				
1. AGENCY USE ONLY (Leave blank)	2. REPORT DATE October 1999	3. REPORT TYPE AND DATES COVERED Annual (26 Sep 98 - 25 Sep 99)		
4. TITLE AND SUBTITLE Thin Film CdZnTe Detector Arrays for Digital Mammography		5. FUNDING NUMBERS DAMD17-96-C-6086		
6. AUTHOR(S) Rengarajan Sudharsanan, Ph.D.				
7. PERFORMING ORGANIZATION NAME(S) AND ADDRESS(ES) Spire Corporation Bedford, Massachusetts 01730-2396		8. PERFORMING ORGANIZATION REPORT NUMBER 10178		
9. SPONSORING/MONITORING AGENCY NAME(S) AND ADDRESS(ES) U.S. Army Medical Research and Materiel Command Fort Detrick, Maryland 21702-5012		10. SPONSORING/MONITORING AGENCY REPORT NUMBER		
11. SUPPLEMENTARY NOTES				
12a. DISTRIBUTION/AVAILABILITY STATEMENT Approved for public release; distribution unlimited		12b. DISTRIBUTION CODE		
13. ABSTRACT (Maximum 200 words) The objective of this program has been to develop large-area, flat-panel detectors for digital mammography using CdTe or CdZnTe deposited by metalorganic chemical vapor deposition (MOCVD) directly on thin-film transistor (TFT) active matrix arrays for image readout. CdTe and CdZnTe have the potential to meet the requirements for digital mammography due to their high x-ray absorption, large band gap and good carrier transport. Activities during the first three years have been directed primarily toward optimization of physical and electrical properties of MOCVD-deposited CdTe and CdZnTe and improved understanding of CdS/Cd(Zn)Te heterojunctions used to reduce the leakage currents. Leakage currents to date have been too high for compatibility with TFT arrays, and this fact has made it impossible to advance to subsequent steps in the program. In the third year our efforts concentrated on transferring growth to a different MOCVD reactor to improve safety and provide the capability for large-area deposition, modeling of absorption efficiency for Cd(Zn)Te compared to alternative materials, and investigation of the possibility of depositing films at low temperature for compatibility with amorphous silicon TFT arrays. Our results indicate that deposition on polysilicon TFTs is the most viable approach, since CdSe TFTs are no longer commercially available.				
14. SUBJECT TERMS CdTe, CdZnTe, array, mammography, MOCVD, TFT, heterojunction		15. NUMBER OF PAGES 37		
		16. PRICE CODE		
17. SECURITY CLASSIFICATION OF REPORT Unclassified	18. SECURITY CLASSIFICATION OF THIS PAGE Unclassified	19. SECURITY CLASSIFICATION OF ABSTRACT Unclassified	20. LIMITATION OF ABSTRACT Unlimited	

FOREWORD

Opinions, interpretations, conclusions, and recommendations are those of the author and are not necessarily endorsed by the U.S. Army.

 X Where copyrighted material is quoted, permission has been obtained to use such material.

 X Where material from documents designated for limited distribution is quoted, permission has been obtained to use the material.

 X Citations of commercial organizations and trade names in this report do not constitute an official Department of Army endorsement or approval of the products or services of these organizations.

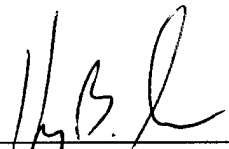
 N/A In conducting research using animals, the investigator(s) adhered to the "Guide for the Care and Use of Laboratory Animals," prepared by the Committee on Care and Use of Laboratory Animals of the Institute of Laboratory Resources, National Research Council (NIH Publication No. 86-23, Revised 1985).

 N/A For the protection of human subjects, the investigator(s) adhered to policies of applicable Federal Law 45 CFR 46.

 N/A In conducting research utilizing recombinant DNA technology, the investigator(s) adhered to current guidelines promulgated by the National Institute of Health.

 N/A In the conduct of research utilizing recombinant DNA, the investigator(s) adhered to the NIH Guidelines for Research Involving Recombinant DNA Molecules.

 N/A In the conduct of research involving hazardous organisms, the investigator(s) adhered to the CDC-NIH Guide for Biosafety in Microbiological and Biomedical Laboratories.



Harvey B. Serreze, Ph.D. 11/12/99
Principal Investigator Date

TABLE OF CONTENTS

	<u>Page</u>
1. COVER PAGE.....	i
2. DOCUMENTATION PAGE (298 FORM).....	ii
3. FOREWORD	iii
4. TABLE OF CONTENTS.....	iv
5. INTRODUCTION	1
6. RESULTS	1
6.1 Review of Program Objectives and Prior Results.....	1
6.2 Third-Year Results.....	3
6.2.1 Refit of MOCVD Reactor	3
6.2.2 Low-Temperature Deposition	4
6.2.3 High-Temperature Deposition	5
6.2.4 Modeling of Absorption Efficiency	8
7. KEY RESEARCH ACCOMPLISHMENTS	9
8. REPORTABLE OUTCOMES.....	9
9. CONCLUSIONS.....	9
10. REFERENCES	10
APPENDIX A - Calculation of Energy Absorption Efficiency for Several X-ray Sources and Absorber Materials	

LIST OF FIGURES

	<u>Page</u>
1 Diagram of the proposed detector concept.	1
2 Diagram of new MOCVD reaction chamber.	4
3 Resistivity as determined by current-voltage measurements for CdZnTe/ITO (open circles) and leakage current for CdZnTe/CdS/ITO (closed circles) versus growth rate at 250°C.	5
4 Reflectance plot for Cd _{1-x} Zn _x Te film on ITO on glass.	6
5 Zinc fraction (solid) and growth rate (dashed) for Cd _{1-x} Zn _x Te on ITO on glass as a function of VI/II flow ratio. Zn/(Zn+Cd) = 0.68, T = 420°C for all	6
6 X-ray spectrum from a tungsten tube at 50 kV constant potential at the tube output (solid) and after attenuation by 5 cm of soft tissue (dotted) ⁵	8
7 Absorption efficiency for x-ray spectra shown in Figure 4 as a function of film thickness for CdTe and Se.	9

LIST OF TABLES

	<u>Page</u>
1 MOCVD Growth Parameters and Film Characteristics	7

5. INTRODUCTION

The most promising approach for improving diagnostic accuracy in x-ray mammography is replacement of film-based systems with digital x-ray imaging systems. Several manufacturers have introduced digital x-ray imaging systems employing amorphous silicon (a-Si) thin-film transistor (TFT) arrays in conjunction with phosphor screens or scintillator crystals that absorb x-rays and emit visible or near-IR light. A photodiode integrated with each TFT converts the light into an electrical signal. The next major step in the development of digital x-ray systems will be replacement of this two-step conversion process by a direct-conversion method, in which a photoconductor absorbs X-rays and generates an electrical signal directly. Several direct-conversion materials have been discussed, including amorphous selenium (a-Se),¹ lead iodide (PbI₂),² mercuric iodide (HgI₂)³ and thallium bromide (TlBr).⁴ Reasonable success has been achieved with each of these materials, but none has the combination of high resistivity and good carrier transport properties required for optimum detection efficiency. We have proposed to deposit cadmium zinc telluride (CdZnTe) on TFT arrays by metalorganic chemical vapor deposition (MOCVD). If properties similar to those of bulk CdZnTe radiation detector crystals can be obtained, this material has the potential for significantly improved x-ray sensitivity over alternative methods.

6. RESULTS

6.1 Review of Program Objectives and Prior Results

The objective of the four-year program addressed in this Third Annual Report is to develop a large-area, flat-panel solid-state X-ray detector for digital mammography using thin-film CdTe or CdZnTe deposited directly on a thin-film transistor (TFT) active matrix array for image readout. To demonstrate this concept, we proposed to fabricate and test a prototype 1024 x 1024 integrated detector array having 50 μm x 50 μm pixels. The array would employ a high resistivity CdTe or CdZnTe semiconductor layer to convert the incident X-rays to electron-hole pairs, and the resulting charge image would be read out digitally by a pixellated TFT array. The detector concept is illustrated in Figure 1.

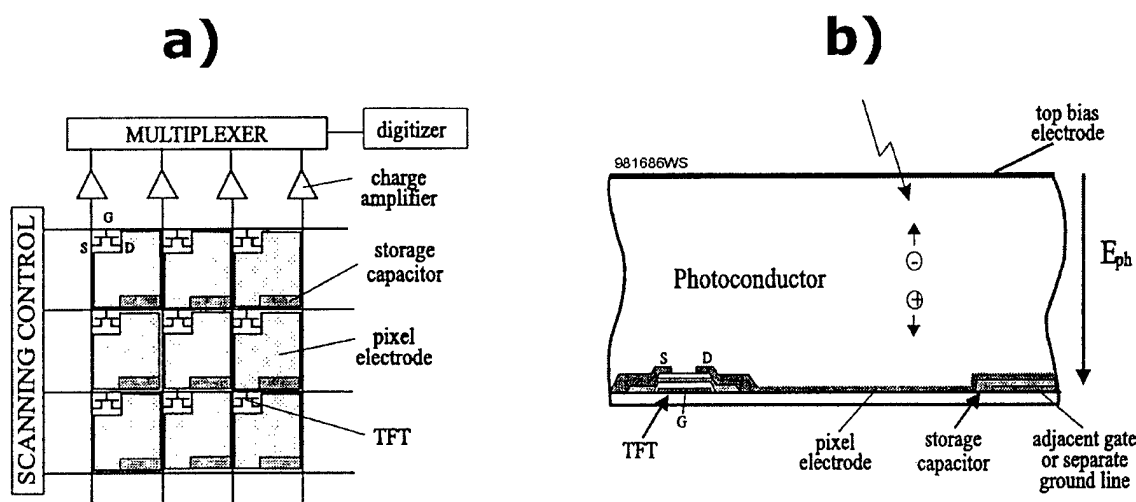


Figure 1 Diagram of the proposed detector concept.

We had planned to develop this detector array in three phases. The first phase was to develop the necessary CdTe or CdZnTe thin films. As part of the effort, we would design and fabricate CdTe or CdZnTe passive matrix detector test arrays with pixel sizes varying from 50 μm to 500 μm on various substrates including glass, gallium arsenide (GaAs), and silicon (Si). Passive matrix detector arrays are relatively simple to fabricate and do not require extensive electronics for testing. These arrays would allow us to measure detection efficiency, signal linearity, pixel size effects, optimum operating voltage, leakage current, and pixel-to-pixel uniformity. The results of these experiments would be used to optimize deposition conditions and detector design parameters. Spire would deposit the films and would design and fabricate the passive matrix detector arrays. Professor John Rowlands from the University of Toronto would characterize the arrays and perform theoretical calculations to determine parameters such as signal level, detection efficiency, X-ray quantum noise, and inherent spatial resolution.

In the second phase we had proposed to integrate prototype CdTe or CdZnTe detector arrays with Si multiplexers. Optimized deposition conditions for the CdZnTe films determined in the first stage were to be employed. A Si multiplexer was selected because of its lower cost than the CdSe TFT arrays ultimately to be used. We had planned to employ a 128 x 128 matrix array with 60 μm center-to-center element spacing. Spire was to deposit the thin films on the Si multiplexers, and the University of Toronto was to test these arrays.

In phase three, once the detector fabrication process and the electronics are determined, we had planned to develop a 5 cm x 5 cm prototype self-scanned detector array by integrating thin-film CdTe or CdZnTe detectors with a CdSe TFT array. The purpose of developing a 5 cm x 5 cm prototype was twofold: first, these arrays would be useful for sterotaxic breast biopsy, and second, they would be a first stage demonstration of an 18 x 24 cm large-area detector suitable for digital mammography. The prototype was to be developed jointly with Professor Rowlands and Litton Systems Canada, Ltd., the only North American vendor of CdSe TFTs, and was planned to have 1024 x 1024 50- μm pixel elements. Spire would deposit the CdZnTe detectors on these TFT arrays. Professor Rowlands, in collaboration with Spire, would assemble and characterize the detector arrays. Finally, phantom images using these arrays were to be obtained to demonstrate the usefulness of this approach for digital mammography.

During the first year, we began initial experiments to deposit and examine CdTe and CdZnTe thin films that would be suitable for X-ray detection. CdTe and CdZnTe thin films were deposited by thermal evaporation and metalorganic chemical vapor deposition (MOCVD) onto a variety of substrates including ITO (indium tin oxide)-coated glass, CdS/ITO-coated glass, GaAs, and plain glass. Samples were characterized for morphology, crystal quality, thickness, and electrical properties. Results indicated that films deposited by MOCVD possessed properties superior to those of evaporated films. Consequently, emphasis was directed toward the MOCVD materials. However, further experiments revealed that even the best MOCVD films still did not possess sufficiently high resistivity to give the necessary low leakage current values required. This problem was partially solved by modifying our original device design to include a CdS/Cd(Zn)Te heterojunction blocking-contact configuration similar to a design we had developed previously. The consequence of these unanticipated problems was that many of the planned materials optimization and array design activities were either not completed or not started according to the original schedule.

During the second year, experiments focused on continuing optimization of the CdTe and CdZnTe films grown by MOCVD. Because of the importance of the material properties in determining the operating characteristics of the final X-ray detector array, it has been necessary to redirect efforts in order to properly address this very crucial issue. Consequently, many of the original tasks focusing on device-related issues (such as preliminary arrays on Si multiplexer arrays) had to be either delayed or canceled. Until material properties are brought to the proper level, it is premature to go to the next steps in the development process.

6.2 Third-Year Results

Experimental efforts in the third year continued to focus on improving the properties of the CdZnTe thin films. Since the current major stumbling block is the insufficient resistivity of the films, and our results from the second year indicated that higher resistivity is obtainable with higher zinc content, we focused some attention on controlling the alloy composition of the CdZnTe films and studying the growth rate as a function of zinc content. Early in 1999 it was decided to transfer CdZnTe growth to a different MOCVD reactor. This change required substantial refitting of the reactor. The change of reactor necessitated substantial re-optimization of growth conditions.

During the most recent report period we became aware that CdSe TFT arrays were no longer commercially available, and it was therefore necessary to consider an alternative. Since the current trend is toward amorphous silicon TFTs we carried out a series of experiments to determine whether CdZnTe thin films could be deposited at sufficiently low temperature ($< 250^{\circ}\text{C}$) for compatibility with a-Si. Since the obtainable growth rate at 250°C is significantly lower than at higher temperatures, we reconsidered the required film thickness to obtain reasonable absorption efficiency for mammography X-rays. Calculations were performed to determine the absorption efficiency as a function of film thickness and alloy composition for CdZnTe films in response to several different x-ray spectra.

During the third year we installed a 75 kVp pulsed x-ray generator to enable on-site testing of x-ray response. We anticipate that in the fourth year of the program this system will be used to compare the x-ray sensitivity of films grown under various conditions and provide additional feedback for optimization of the films.

6.2.1 Refit of MOCVD Reactor

Optimal use of Spire's MOCVD laboratory facilities in service of its several research programs dictated that II-VI materials growth be transferred to a different reactor than the one that was used during the previous two years. The reactor which was designated as the new II-VI machine had been a multi-wafer reactor which was originally used for CdZnTe growth on Si and GaAs wafers. More recently this system had been used for growth of GaAs solar cells. The new reactor also possessed a number of safety features that had become necessary. The reactor design totally separates the pumping area from the loading area and it utilizes an all-welded exhaust system; these improved fume-control features greatly reduced the likelihood of Cd and Te exposure to the operator which had started to become a problem on the previous machine. Finally, the new reactor is located in a Class 100 laboratory compared to a localized Class 100 loading area within a Class 10,000 laboratory for the old system. This feature helped reduce particulate contamination to the films. Although these improvements contributed to a slight program delay, we believe that they were in the best interest of the program.

Because it was not economically feasible to operate the reactor in its multi-wafer configuration for this program, a new, smaller reaction chamber was built. This chamber uses a glass bell jar and did not originally incorporate rotation of the substrate. After initial growth runs indicated poor thickness uniformity over the substrate area, a gear mechanism was added to rotate the susceptor. This measure greatly improved the film uniformity. A quartz cover was placed over the gears to protect them from contamination. A diagram of the reaction chamber is shown in Figure 2.

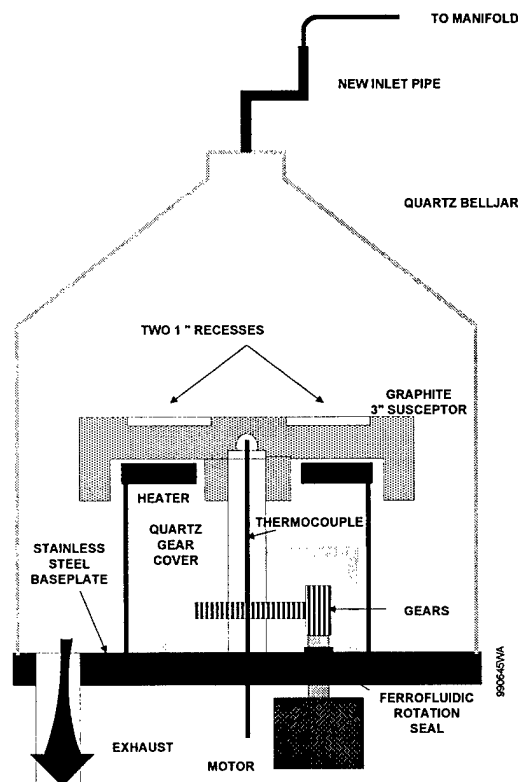


Figure 2 **Diagram of new MOCVD reaction chamber.**

The properties of the films grown in this system have not reached the level of those from the previous system. Leakage currents at a bias of $0.5 \text{ V}/\mu\text{m}$ typically have been several hundred nA per mm^2 and in some cases have reached the mA level. Furthermore, adhesion of the film to the ITO/glass substrates has been problematic. More work is required to improve the properties of this films grown in this system.

6.2.2 Low-Temperature Deposition

Since CdSe TFT arrays are no longer available, and a-Si:H TFTs are one alternative, we performed a series of experiments to determine whether adequate growth rate and film quality could be achieved at a growth temperature of 250°C - the maximum to which a-Si:H can be subjected without rapid degradation. These experiments were funded by a commercial customer at no cost to this program. We include the results here to present a more complete picture of current status and future prospects for CdZnTe thin-film x-ray detectors.

In order to improve the growth rate at low temperature, an alternative tellurium source, diallyltellurium(DATe) was used in place of the usual dimethyl tellurium (DMTe). Even so, the growth rate was an order of magnitude lower than typically achieved at $400\text{--}450^\circ\text{C}$. Furthermore, the resistivity of the films was much lower than at higher growth temperature. A number of different growth conditions were used, and films were deposited both on ITO and on CdS/ITO, the latter forming a heterostructure which often provides lower leakage current. The salient results are summarized in Figure 3, which gives the resistivity as determined by I-V measurements for CdZnTe/ITO films and the leakage current for CdZnTe/CdS/ITO. Unfortunately, the resistivity tends to decrease as the growth rate increases. There is no clear trend for the leakage current of CdZnTe/CdS/ITO as a function of growth rate.

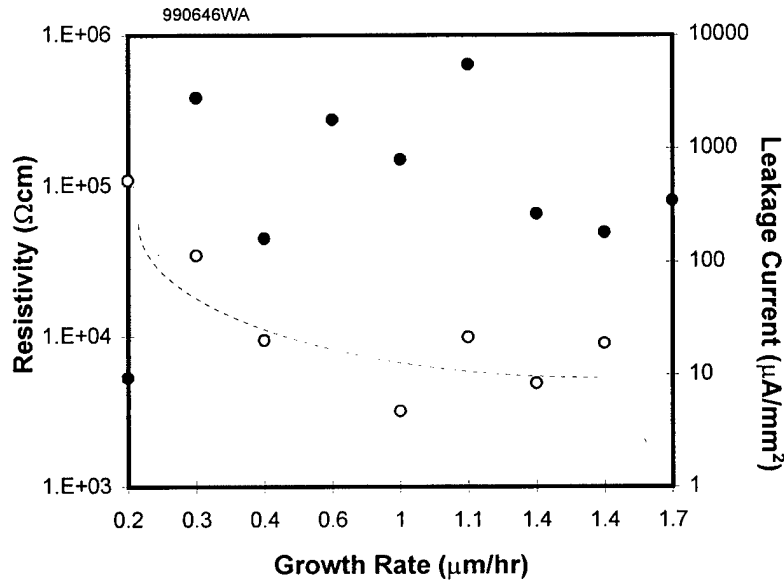


Figure 3 Resistivity as determined by current-voltage measurements for CdZnTe/ITO (open circles) and leakage current for CdZnTe/CdS/ITO (closed circles) versus growth rate at 250°C.

The conclusion that must be drawn from these experiments is that both the growth rate and the electrical properties of the films grown at 250°C are unacceptable. Hence deposition of CdZnTe films on a-Si TFTs by MOCVD appears not to be practical.

6.2.3 High-Temperature Deposition

We conducted a number of runs in the refurbished reactor at a temperature of 420-440°C, which was the optimal range in the previous reactor. The first few runs were conducted using DATe as the Te source. We discovered, however, that this precursor gives poor growth rates in this temperature range, typically 1-3 μm/hr. We therefore reverted to dimethyl tellurium (DMTe), which gave much higher growth rates, approximately 15 μm/hr for CdTe, but somewhat lower for CdZnTe. A series of runs were performed in which the VI/II flow ratio was varied.

Our previous results have shown that the electrical properties of the films may depend strongly on the alloy composition. In particular, higher resistivity is often obtained with Zn-rich films. It was important therefore to understand how the composition and growth rate depend on the flow rates of the precursors. To characterize this property we carried out several runs at fixed Cd and Zn flow rates while varying the Te flow rate. The temperature was fixed at 420°C. The composition of each film was determined from reflectance measurements, an example of which is shown in Figure 4. The linearly rising portion of the curve is extrapolated back to determine the x-intercept. This wavelength, λ_c , is taken to correspond to the band gap, E_g , through the relation:

$$E_g = \frac{hc}{\lambda_c}$$

where h is Planck's constant and c is the speed of light in vacuum. The alloy composition is then determined from:⁵

$$E_g(x) = 1.51 + 0.606x + 0.139x^2$$

As shown in Figure 5, as the Te flow was increased the growth rate increased, but the Zn content decreased.

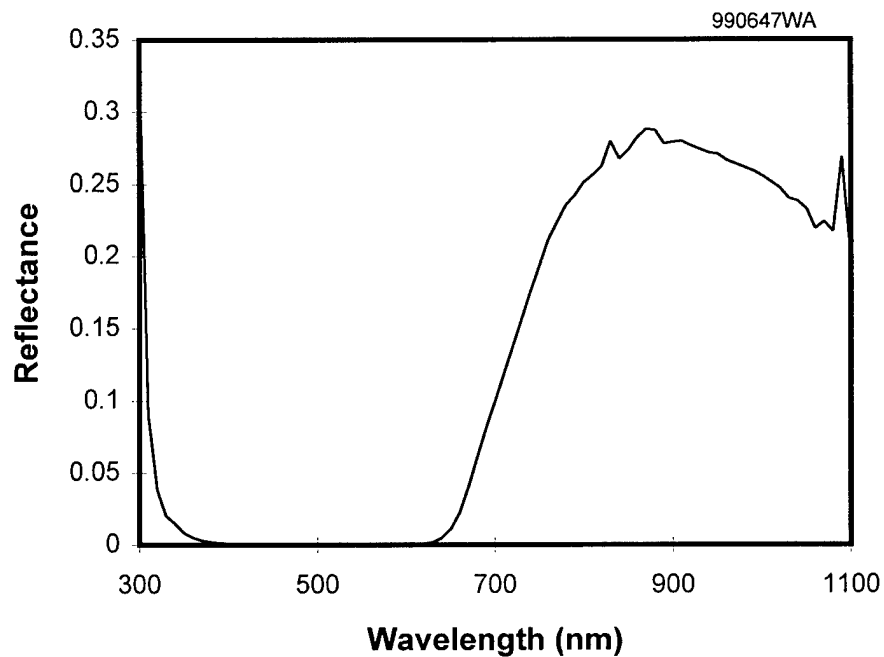


Figure 4 Reflectance plot for $\text{Cd}_{1-x}\text{Zn}_x\text{Te}$ film on ITO on glass.

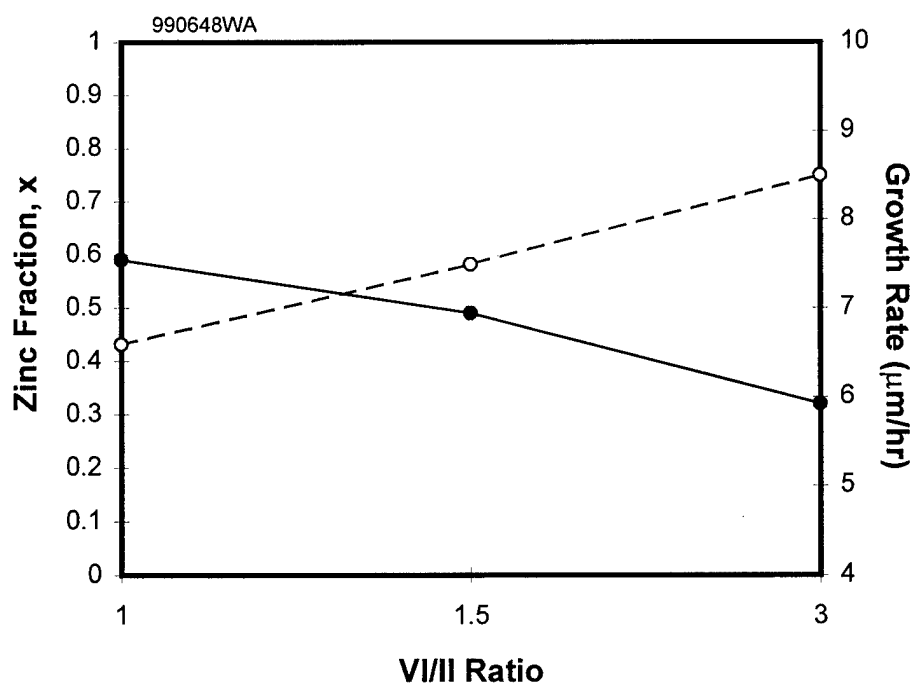


Figure 5 Zinc fraction (solid) and growth rate (dashed) for $\text{Cd}_{1-x}\text{Zn}_x\text{Te}$ on ITO on glass as a function of VI/II flow ratio. $\text{Zn}/(\text{Zn}+\text{Cd}) = 0.68$, $T = 420^\circ\text{C}$ for all.

Table 1 summarizes the results of both the high-temperature and low-temperature runs. In many cases, electrical measurements were not possible because the film failed to adhere to the substrate. It has not yet been determined whether this problem is due to high particulate or contaminant levels in the reactor or to degradation of the substrates in storage.

Table 1 MOCVD Growth Parameters and Film Characteristics

Structure	Substrate Temp (°C)	VI/II Ratio	Zn (Zn+Cd) Flow Ratio	Growth Rate (μm/hr)	Te Source	[Zn]	I(CdS) (nA)	I(ITO) (nA)
CdTe	420	0.7	0	17.1	DMTe			
CdTe	250	0.5	0	1.2	DATe			
CdZnTe	250	0.5	0.295		DATe			
CdTe	250	0.3	0	1.2	DATe			
CdZnTe	250	0.1	0.538	2.0	DATe			
CdZnTe	250	0.8	0.627	1.2	DATe			
CdZnTe	250	0.6	0.618	1.3	DATe			
ZnTe	250	0.3	1.0	0.2	DATe			
CdZnTe	250	5.6	0.622	1.0	DATe			
CdZnTe	250	1.7	0.606	0.5	DATe			
CdTe	440	1.1	0	1.6	DATe			
CdZnTe	440	0.4	0	0.6	DATe		N/A	22,000
CdTe	440	0.4	0	1.2	DATe		9.1	3.7x10 ⁶
CdTe	440	0.4	0		DATe		180	N/A
CdTe	440	0.4	0	5.5	DATe			
CdTe	440	0.5	0		DATe			
CdTe	440	0.4	0		DATe			
*CdTe	440	0.8	0	0.7	DATe			
CdTe	420	0.7	0	17.7	DMTe			
CdTe	420	0.7	0	16.2	DMTe			
CdTe	420	0.7	0	17.0	DMTe			
CdZnTe	420	1.0	0.677	13.2	DMTe	0.59		
CdZnTe	420	1.5	0.677	15.0	DMTe	0.49		
CdZnTe	420	3.0	0.677	17.0	DMTe	0.32		

* First run with rotating susceptor

6.2.4 Modeling of Absorption Efficiency

A typical x-ray spectrum used for mammography (50 kV, tungsten with 1.0 mm Be / 0.5 mm Al filter) is shown in Figure 6 both as it emerges from the x-ray tube and after attenuation by 5 cm of soft tissue.⁶ While the spectrum that emerges from the tube is concentrated below 25 keV, the spectrum that reaches the detector is significantly hardened, so that the content between 30 and 50 keV makes a major contribution.

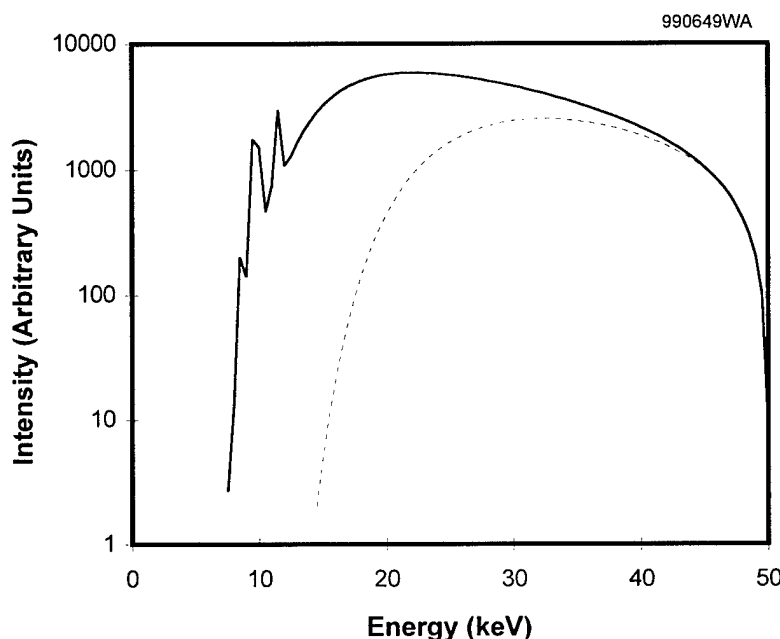


Figure 6 X-ray spectrum from a tungsten tube at 50 kV constant potential at the tube output (solid) and after attenuation by 5 cm of soft tissue (dotted).⁵

We have calculated the energy absorption efficiency as a function of film thickness for these spectra using the equation:

$$\eta = \frac{\int_0^{\infty} (1 - e^{-\alpha(E)d}) g(E) E dE}{\int_0^{\infty} g(E) E dE}$$

where $\alpha(E)$ is the attenuation coefficient for photons of energy E ,⁷ $g(E)$ is the spectral density plotted in Figure 6, and d is the detector thickness. The results are shown in Figure 7, both for CdTe and selenium. The horizontal axis is in units of g/cm^2 , so that the actual film thickness is obtained by dividing by the density of the material ($5.87 g/cm^3$ for CdTe, $4.3 g/cm^3$ for a-Se). CdTe has significantly higher absorption efficiency than a-Se for a given film thickness, especially for the spectrum as hardened by soft tissue absorption. The CdTe film thickness required for 90 % absorption efficiency is approximately $200 \mu m$, compared to more than $600 \mu m$ for a-Se. This result implies that the growth rates obtained by MOCVD in the $400-500^\circ C$ range ($\approx 10-20 \mu m/hr.$) are acceptable, but that the growth rate at $250^\circ C$ ($\approx 1 \mu m/hr.$) is not practical for depositing films of sufficient thickness for x-ray detection. Similar calculations were performed for higher X-ray energies; results are given in Appendix A.

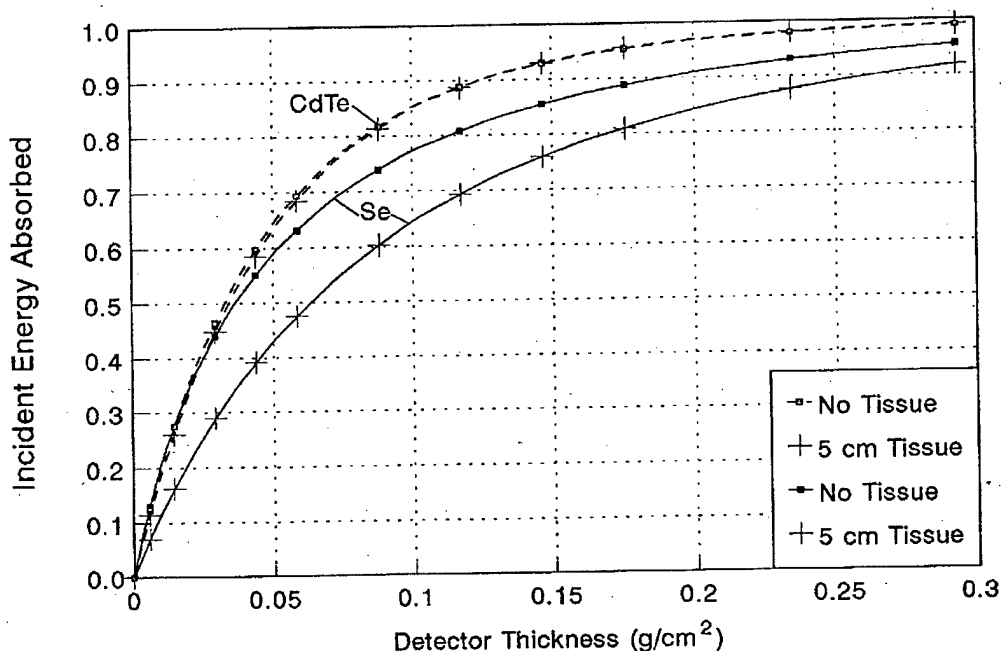


Figure 7 Absorption efficiency for x-ray spectra shown in Figure 4 as a function of film thickness for CdTe and Se.

7. KEY RESEARCH ACCOMPLISHMENTS

- refit of MOCVD reactor
- modeling of absorption efficiency
- characterization of composition and growth rate vs. VI/II ratio
- Installation of X-ray generator

8. REPORTABLE OUTCOMES

There have been no reportable outcomes from this program during the third year.

9. CONCLUSIONS

During Year 3, work continued to better understand and improve the MOCVD thin films of CdTe and CdZnTe needed for the mammography imaging arrays. Results indicate that the leakage currents are still too high in spite of the use of a CdS/CdTe or CdS/CdZnTe heterostructure. At this point, it is not certain whether the high currents are due primarily to film purity or to grain boundary effects. It is imperative that this problem be solved before the program embarks on deposition of films on active device structures such as TFT arrays. Film improvement will therefore be the primary focus for the coming year.

The lack of availability of CdSe TFT arrays has forced us to consider alternative readout systems. The most widely used alternative, a-Si, is impractical because of temperature limitations. It appears therefore that polysilicon TFT arrays would be the most promising approach.

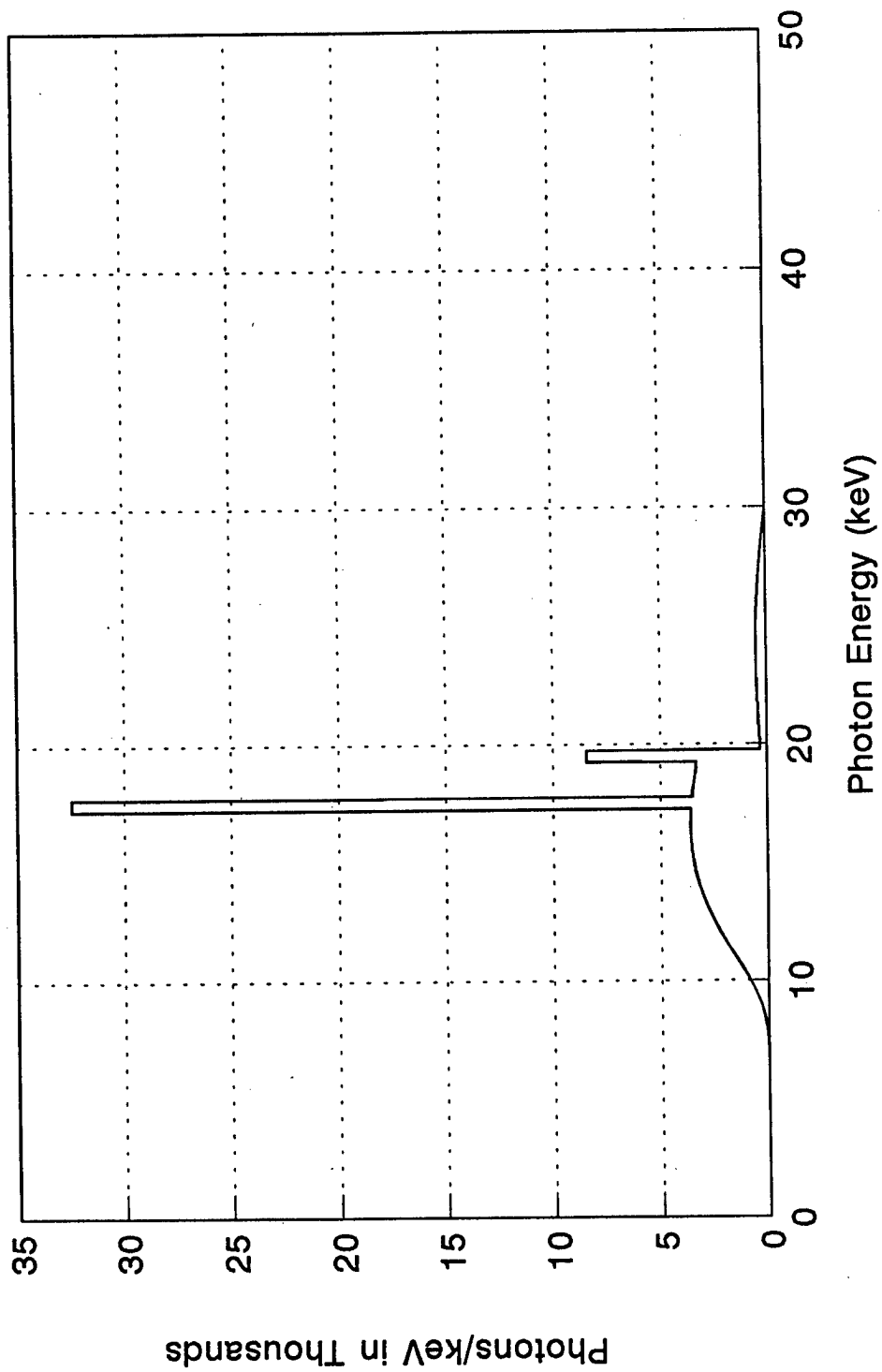
In light of the disappointing results to date of it will be necessary to amend the statement of work formally to reflect a realistic course of action for the final year. The first priority must be to carry out further growth experiments to improve the adhesion and increase the resistivity of the films. Should adequate progress be made, it will then be feasible to perform a deposition on a small polysilicon TFT array and test the response of individual pixels. It does not appear that the remaining time and resources will permit development of a prototype x-ray imaging system. We have identified a university subcontractor that would be able to supply us with prototype polysilicon TFT arrays.

10. REFERENCES

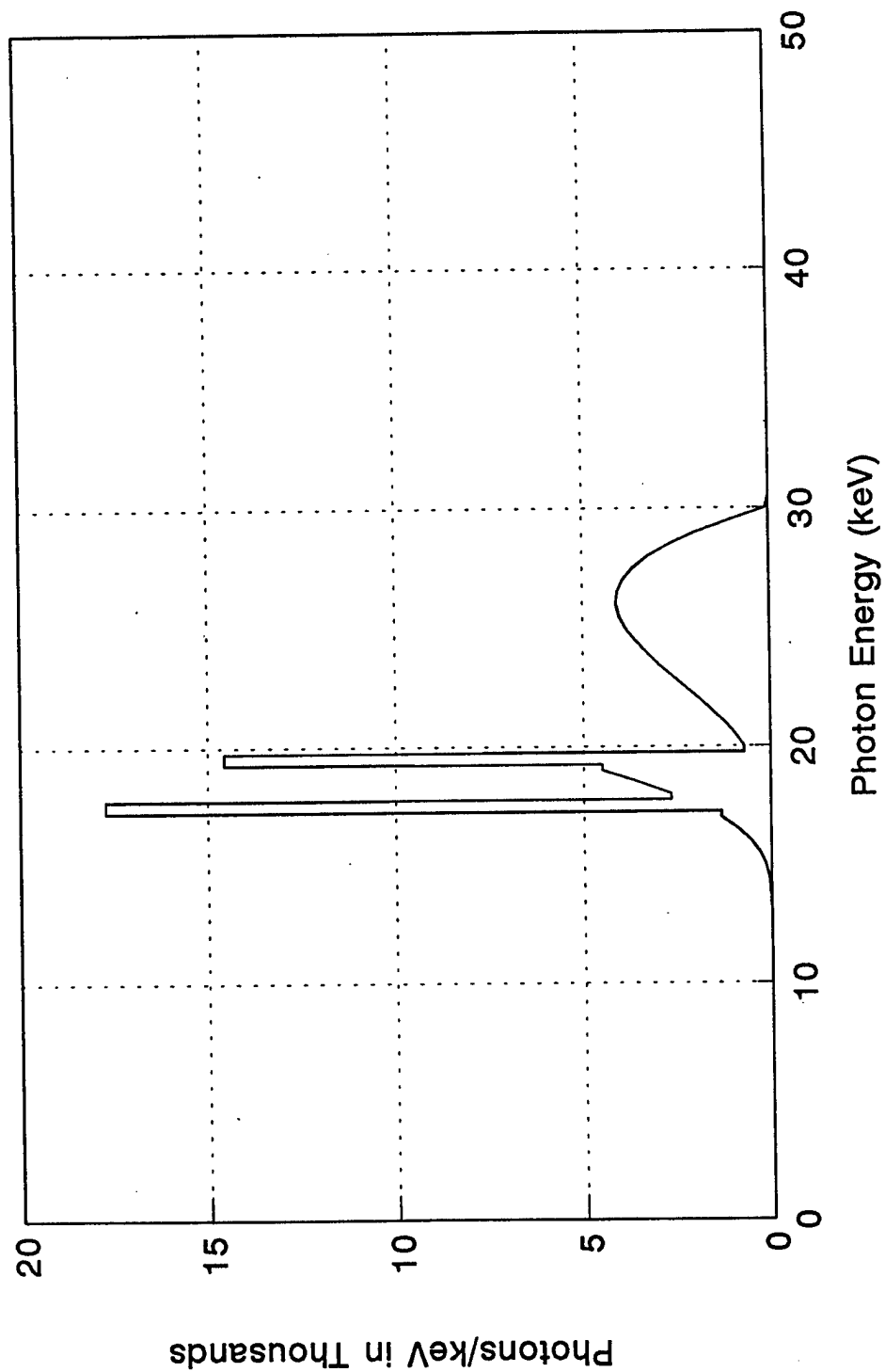
1. W. Zhao, I. Blevis, S. Germann, J.A. Rowlands, D. Waechter and Z. Huang, "Digital Radiology using Active Matrix Readout of Amorphous Selenium: Construction and Evaluation of a Prototype Real-time Detector," *Med. Phys.* **24**, 1834 (1997).
2. K. S. Shah, P. Bennett, Y. Dmitriyev, L. Cirignano, M. Klugerman, M.R. Squillante, R.A. Street, J.T. Rahn and S.E. Ready, "PbI₂ for High Resolution Digital X-ray Imaging," *SPIE Proc.* **3770**, 164 (1999).
3. M. Schieber, H. Hermon, A. Zuck, A. Vilensky, L. Melekhov, R. Shatunovsky, E. Meerson and H. Saado, "Polycrystalline Mercuric Iodide Detectors," *SPIE Proc.* **3770**, 146 (1999).
4. D.R. Ouimette, R.M. Iodice, P-J Kung and L. Lynds, "A Real-time X-ray Image Sensor Using a Thallium Bromide Photoconductor," *SPIE Proc.* **3770**, 156 (1999).
5. Oettinger, K., Hofmann, D.M., Efros, A.L., Meyer, B.K., Salk, M. and Benz, K.W., *J. Appl. Phys.* **71**, 4523 (1992).
6. R. Birch and M. Marshall, "Catalogue of Spectral Data for Diagnostic X-rays," Hospital Physicists Association (1979).
7. E. Storm and I. Israel, "Photon Cross Sections from 0.001 to 100 MeV for Elements 1 through 100," Los Alamos Scientific Laboratory Report LA-3753 (1967).

APPENDIX A
Calculation of Energy Absorption Efficiency for Several X-ray Sources and
Absorber Materials

30 kV CONSTANT POTENTIAL X-RAY SPECTRUM
Molybdenum Target 1.0 mm Be 0.03 mm Mo

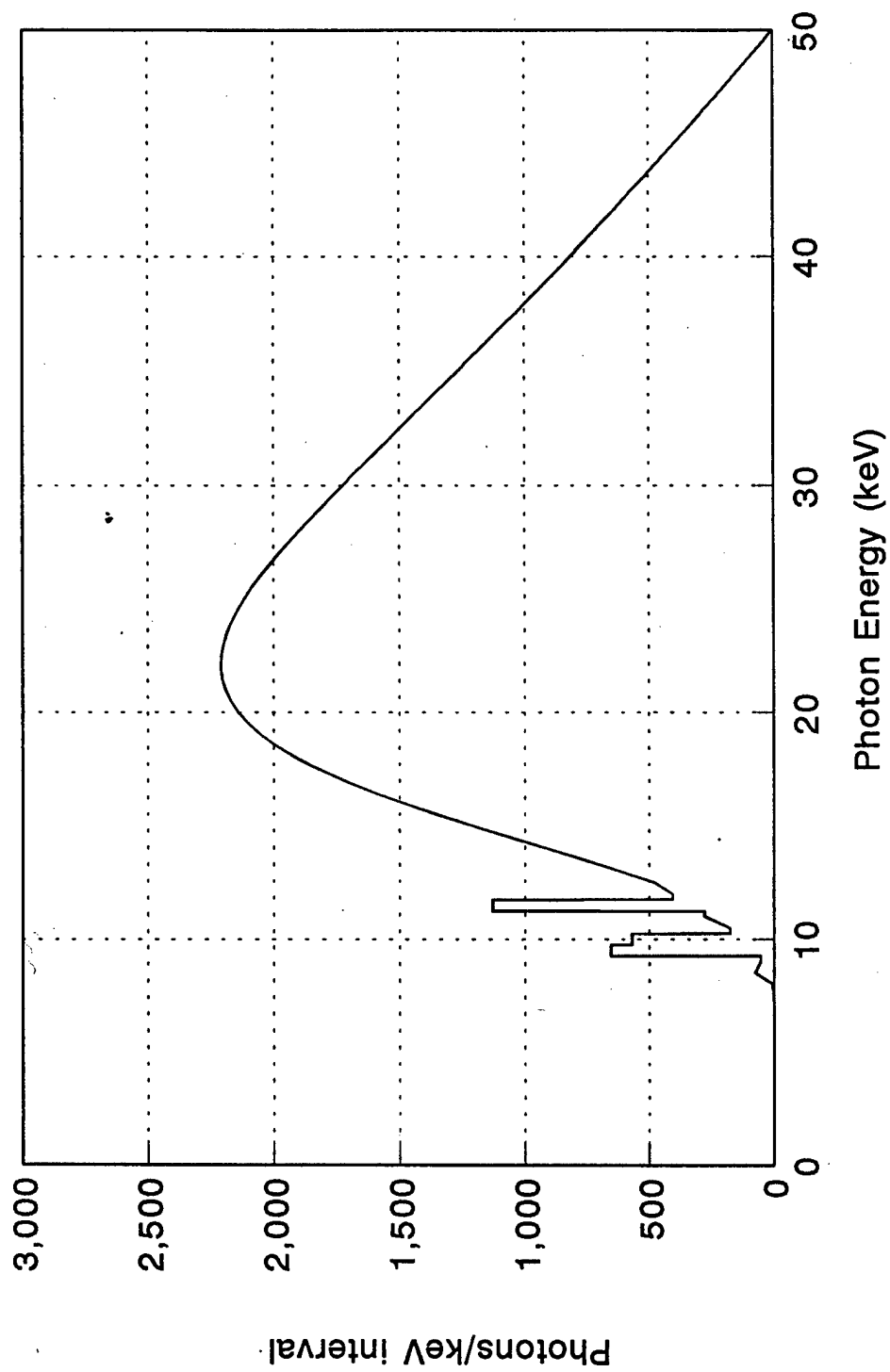


30 kV CONSTANT POTENTIAL X-RAY SPECTRUM
Molybdenum Target 1.0 mm Be 0.03 mm Mo 5.0 cm Tissue

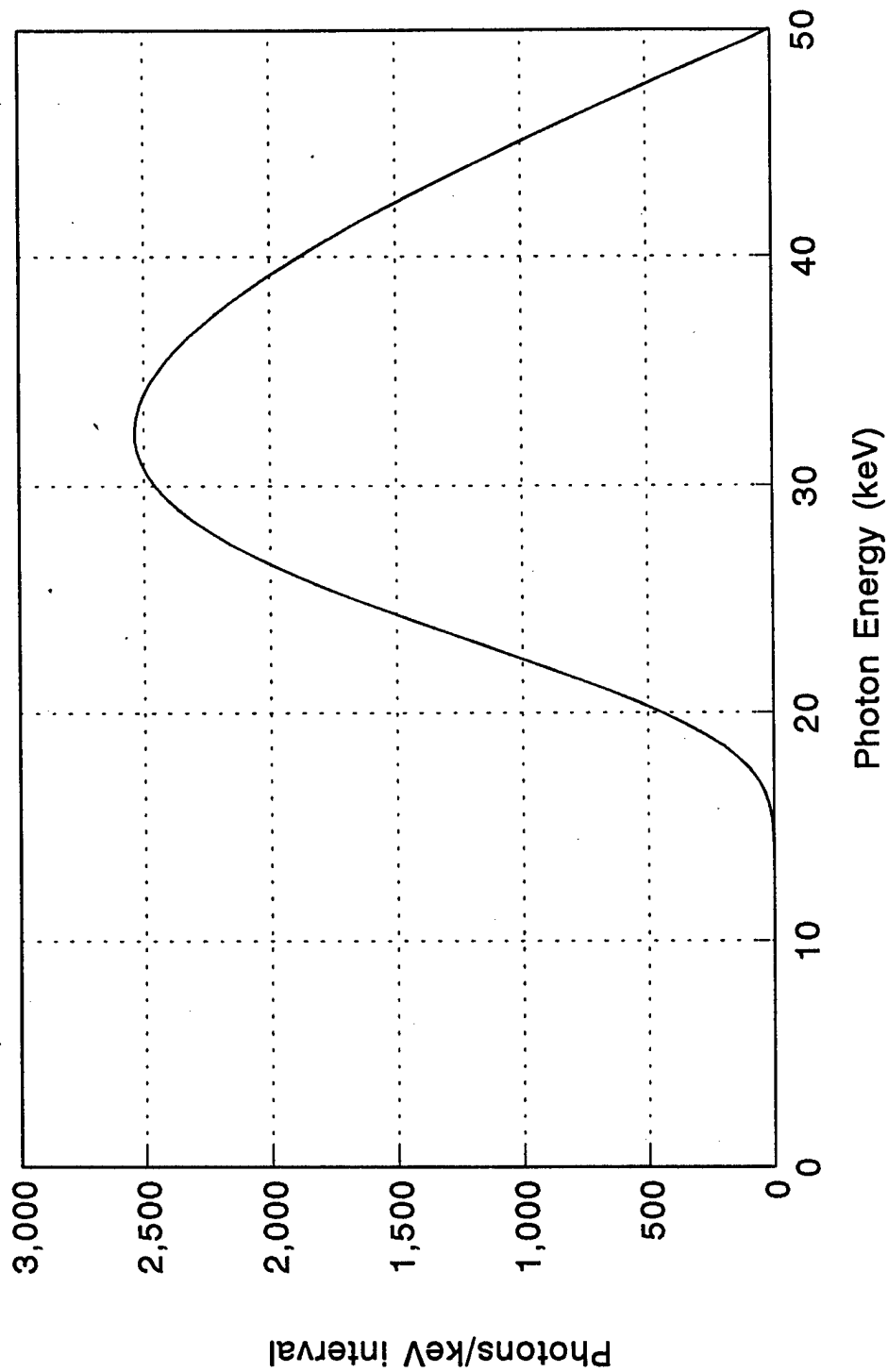


50 kV CONSTANT POTENTIAL X-RAY SPECTRUM

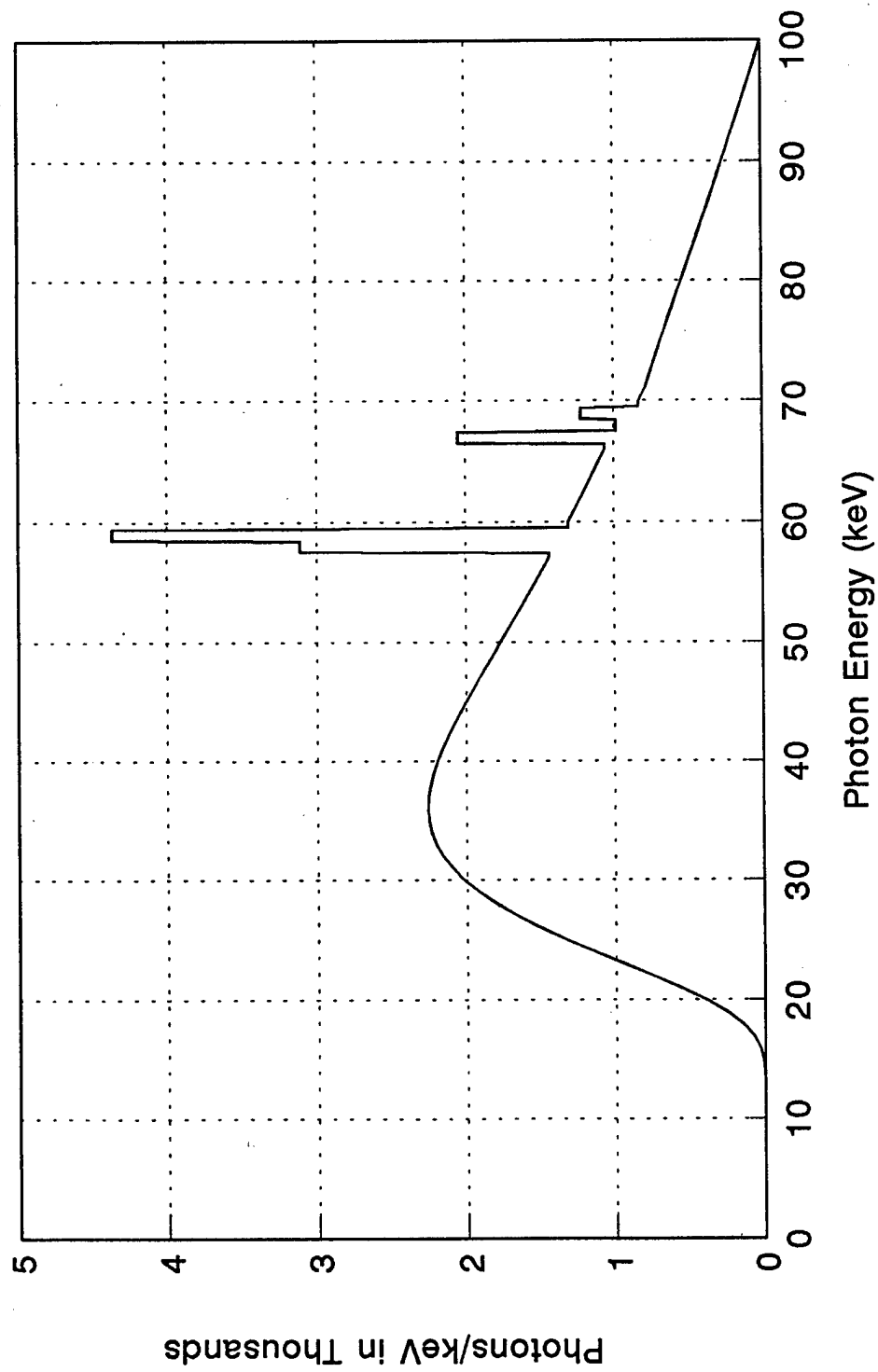
Tungsten Target 1.0 mm Be 0.5 mm Al



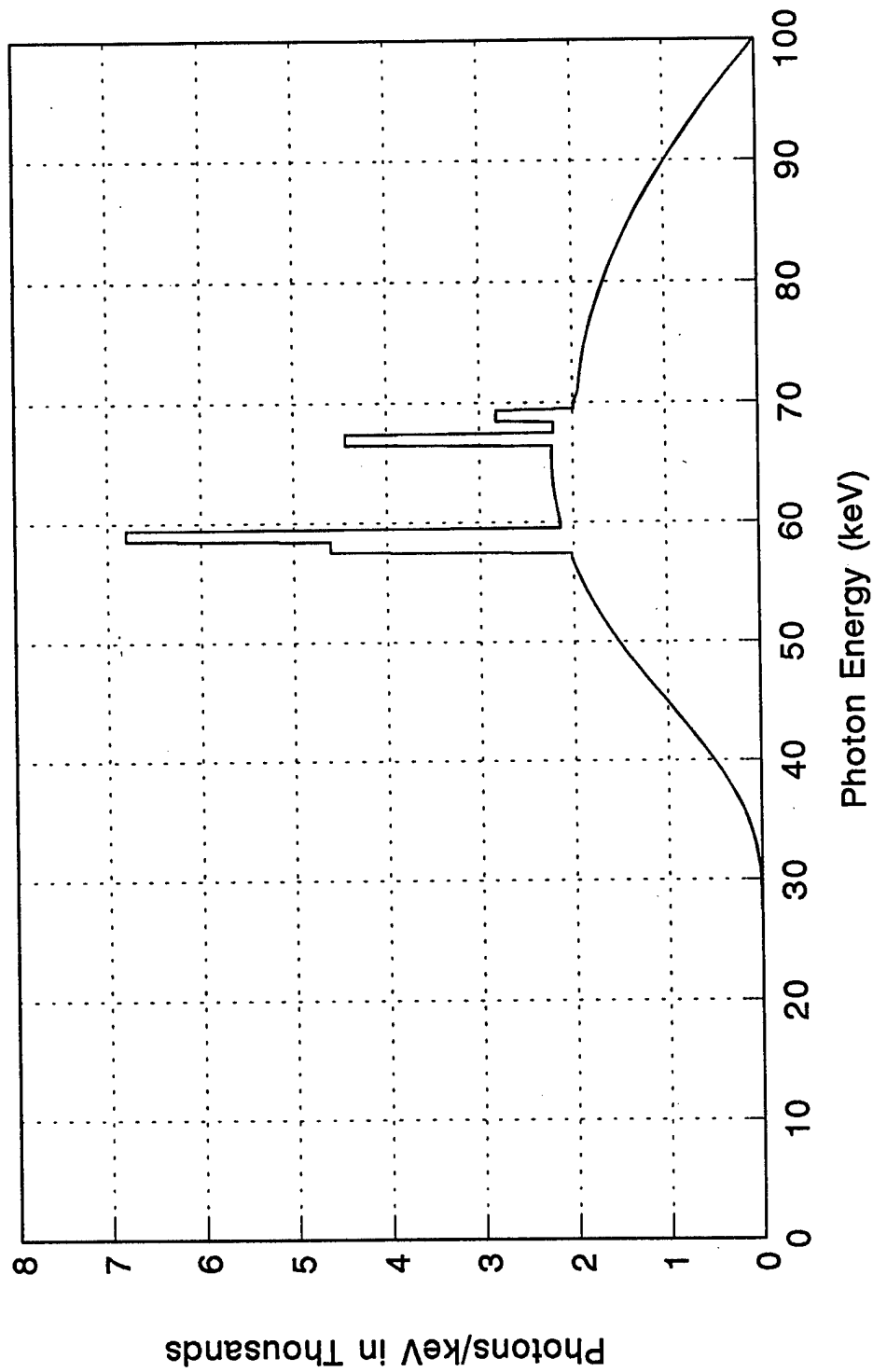
50 kV CONSTANT POTENTIAL X-RAY SPECTRUM
Tungsten Target 1.0 mm Be 0.5 mm Al 5 cm Tissue



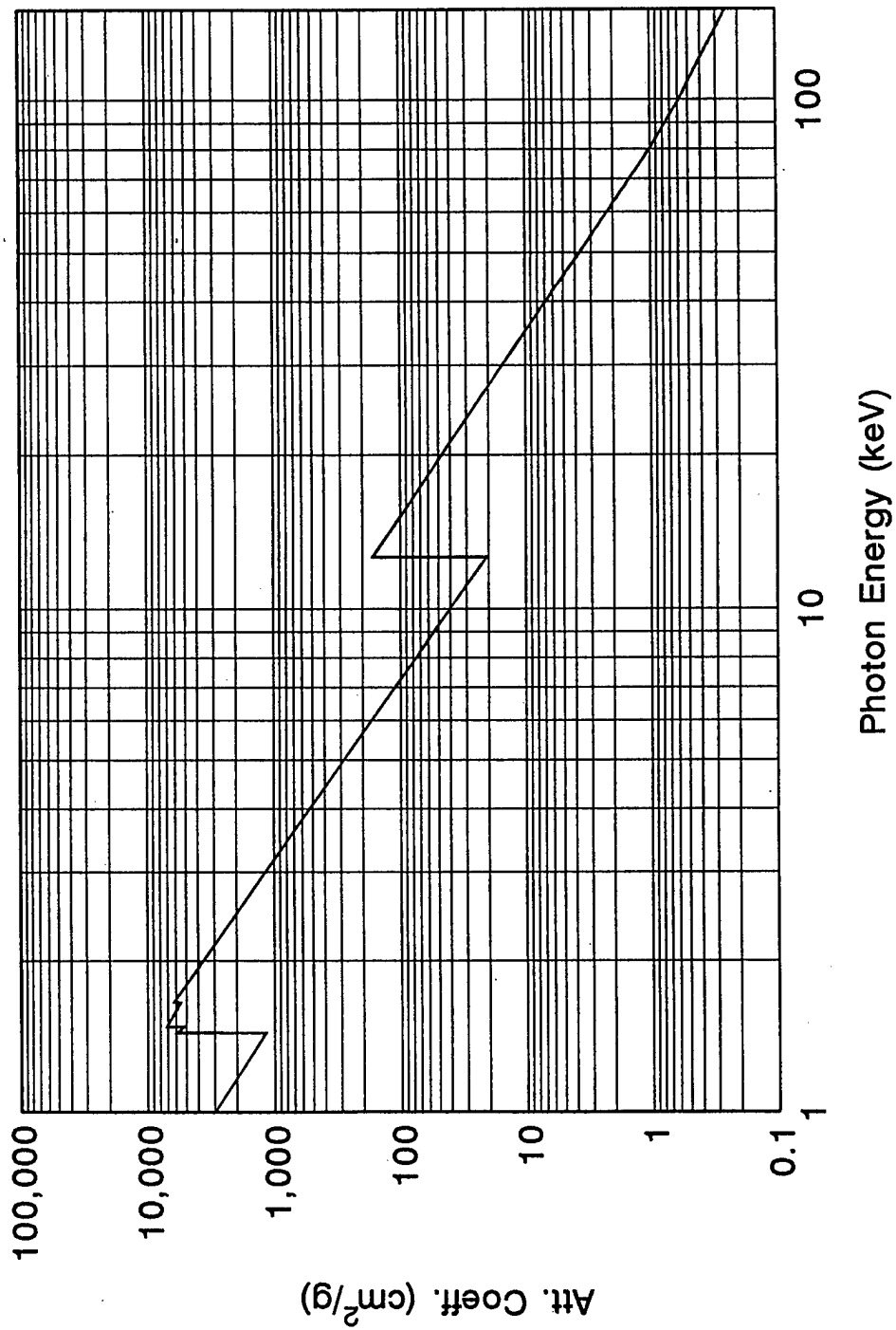
100 kV CONSTANT POTENTIAL X-RAY SPECTRUM
Tungsten Target 2.5 mm Al



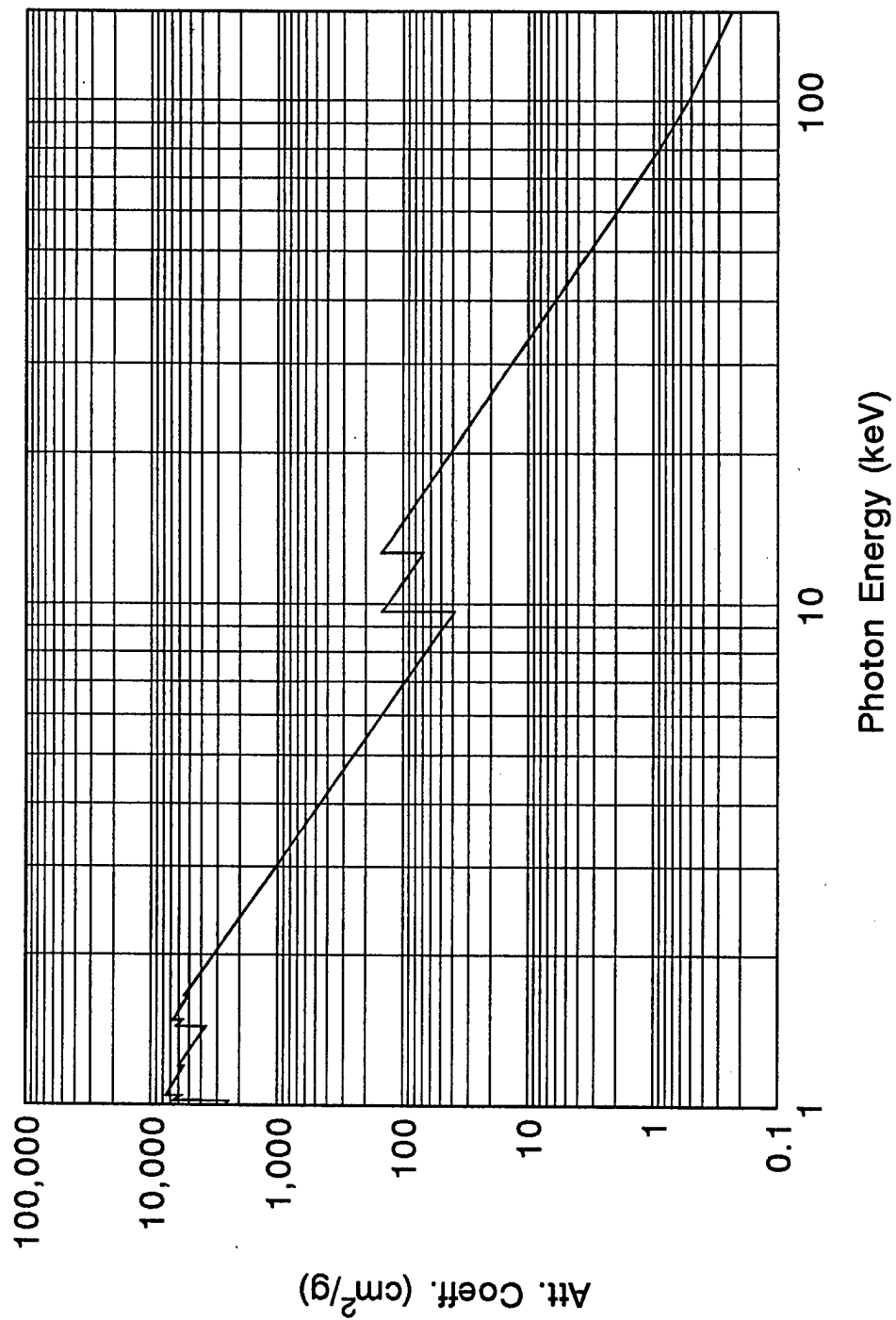
100 kV CONSTANT POTENTIAL X-RAY SPECTRUM
Tungsten Target 2.5 mm Al 18.5 cm Tissue + 1.5 cm Bone



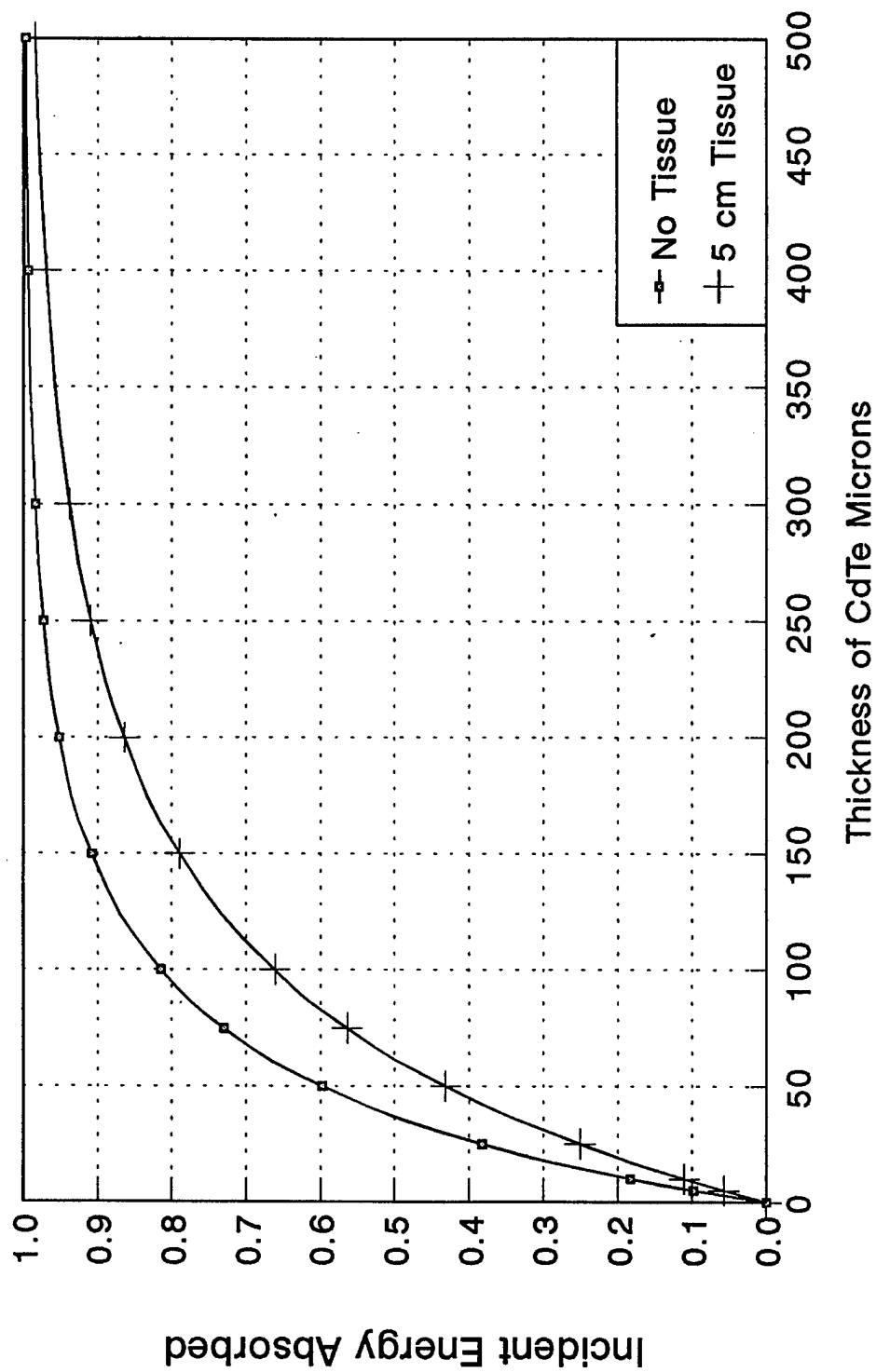
X-RAY ATTENUATION COEFFICIENTS
Selenium Storm and Israel LA-3753 (1967)



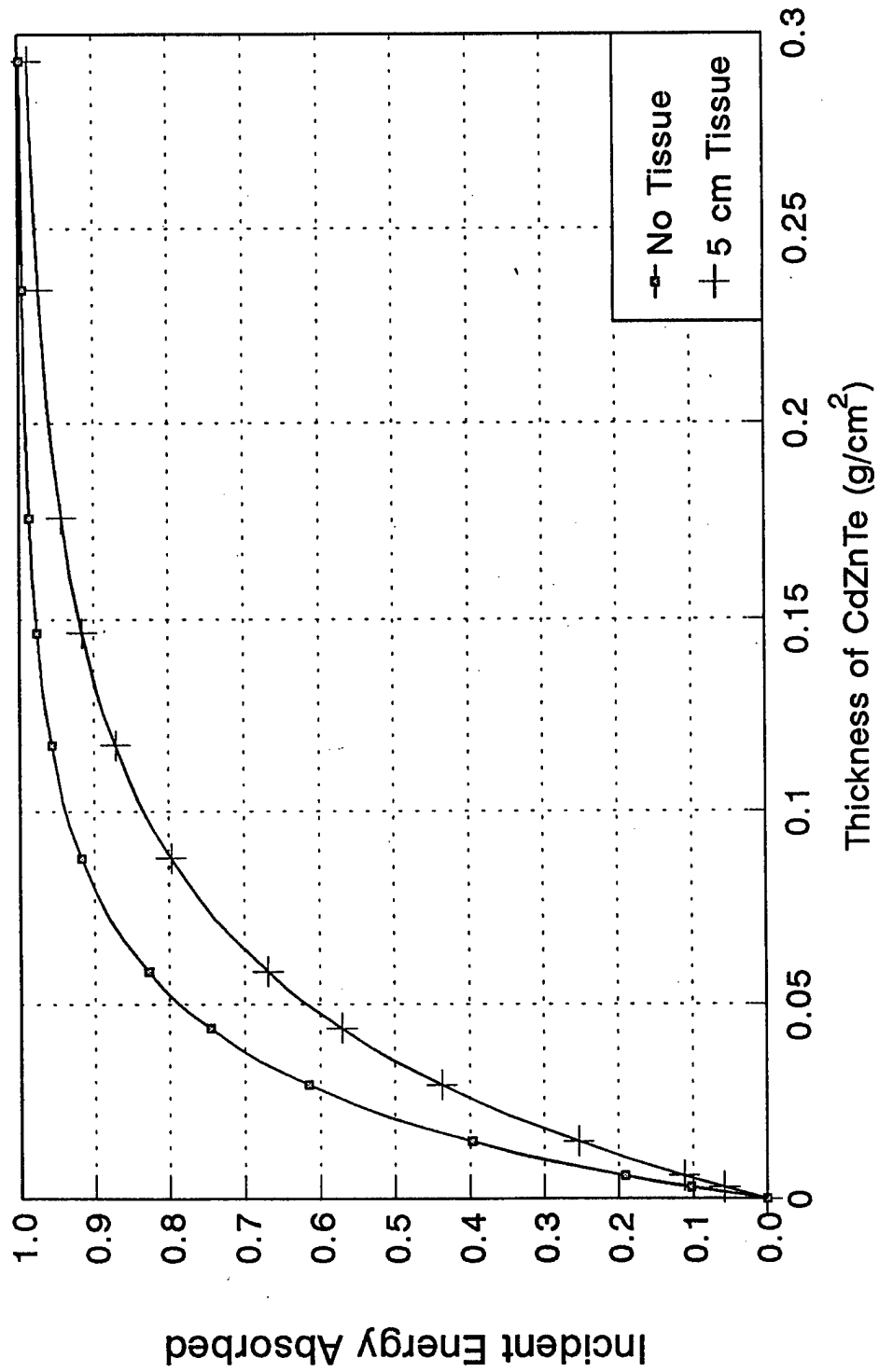
X-RAY ATTENUATION COEFFICIENTS
ZeSe Storm and Israel LA-3753 (1967)



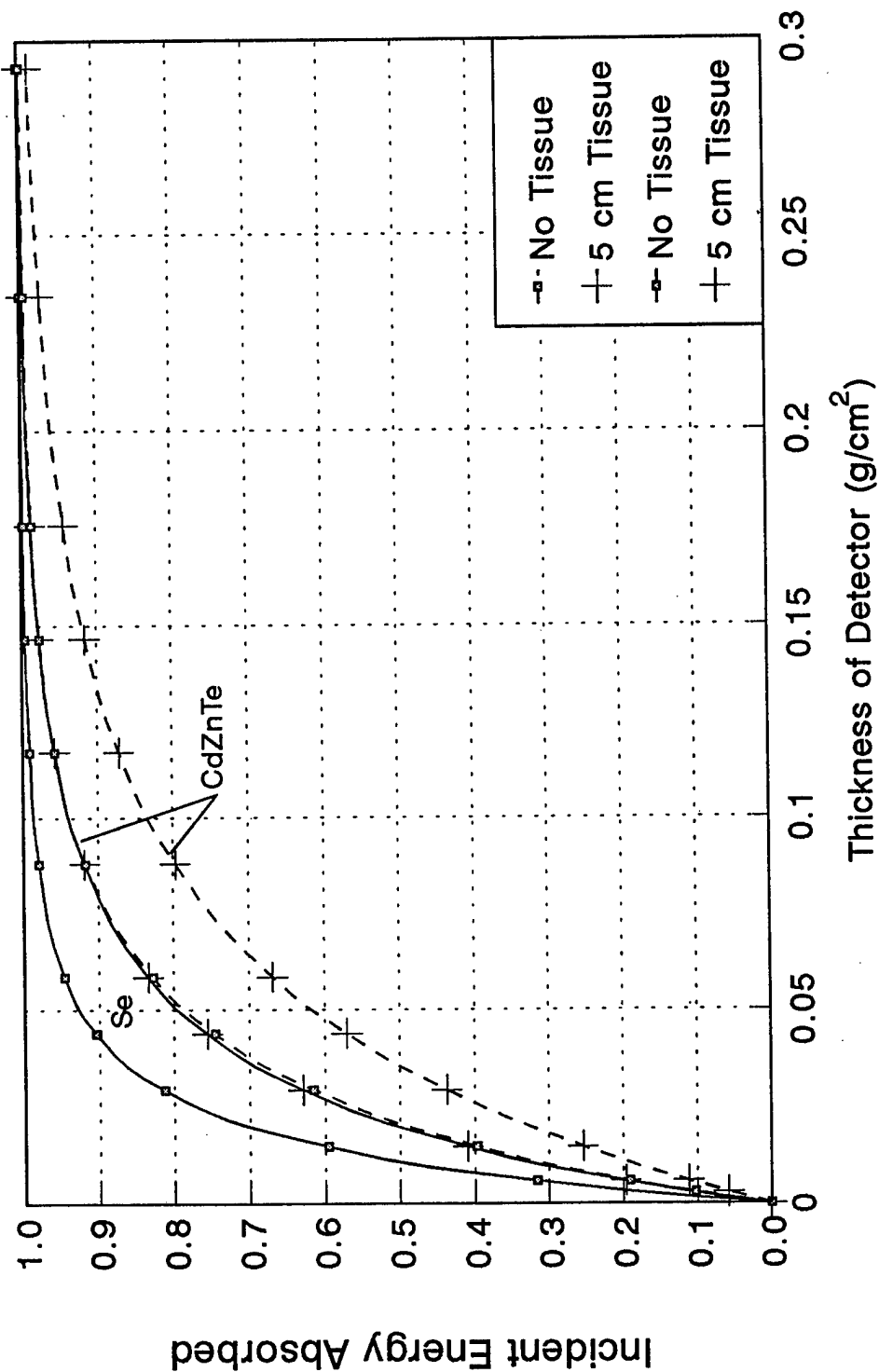
ENERGY DEPOSITION IN CdTe AS A FUNCTION OF THICKNESS
30 kV Molybdenum Spectrum 1.0 mm Be 0.03 mm Mo



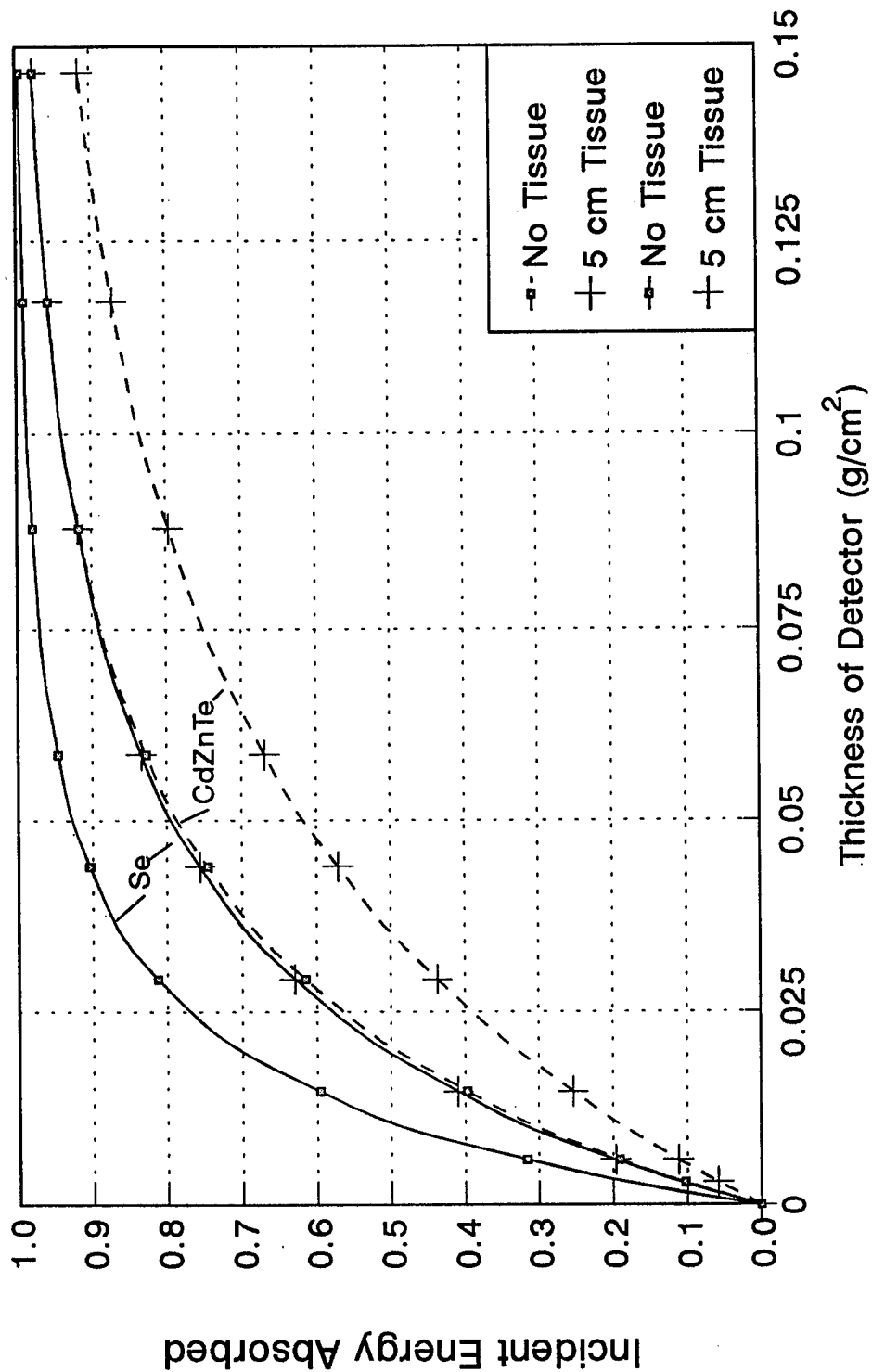
ENERGY DEPOSITION IN CdZnTe AS A FUNCTION OF THICKNESS
30 kV Molybdenum Spectrum 1.0 mm Be 0.03 mm Mo



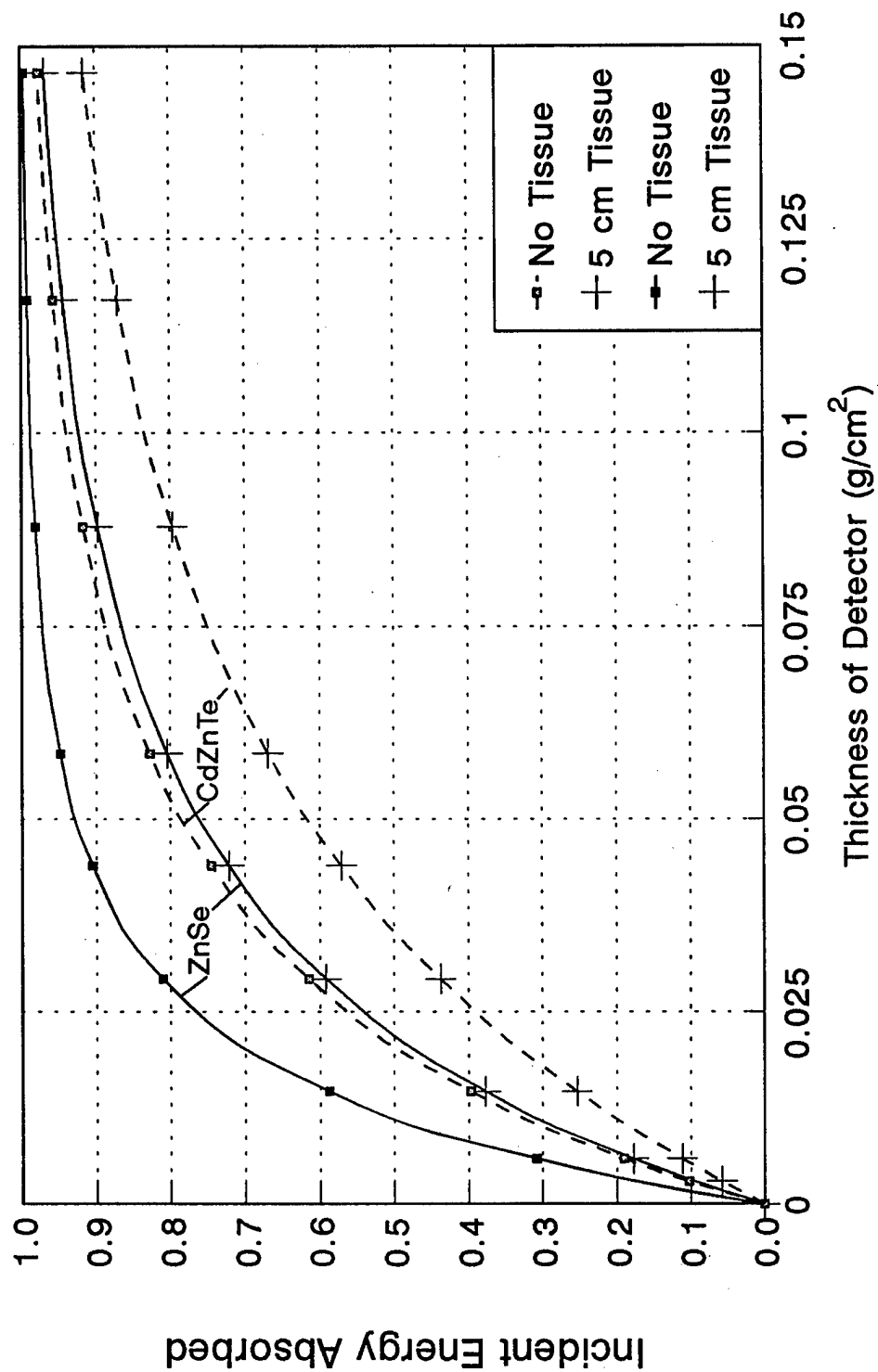
ENERGY DEPOSITION IN CdZnTe AND Se AS A FUNCTION OF THICKNESS 30 kV Molybdenum Spectrum 1.0 mm Be 0.03 mm Mo



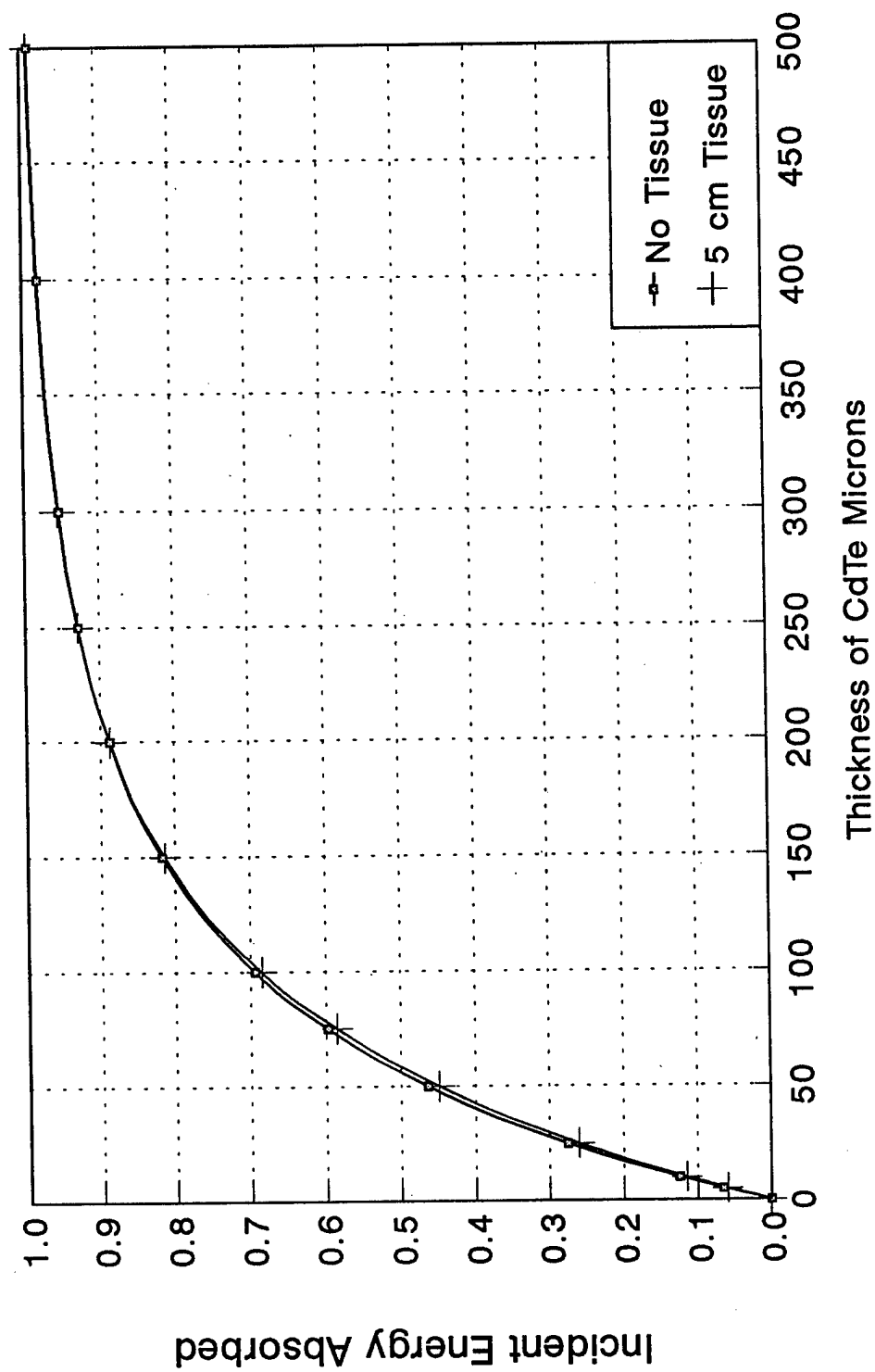
ENERGY DEPOSITION IN CdZnTe AND Se AS A FUNCTION OF THICKNESS
30 kV Molybdenum Spectrum 1.0 mm Be 0.03 mm Mo



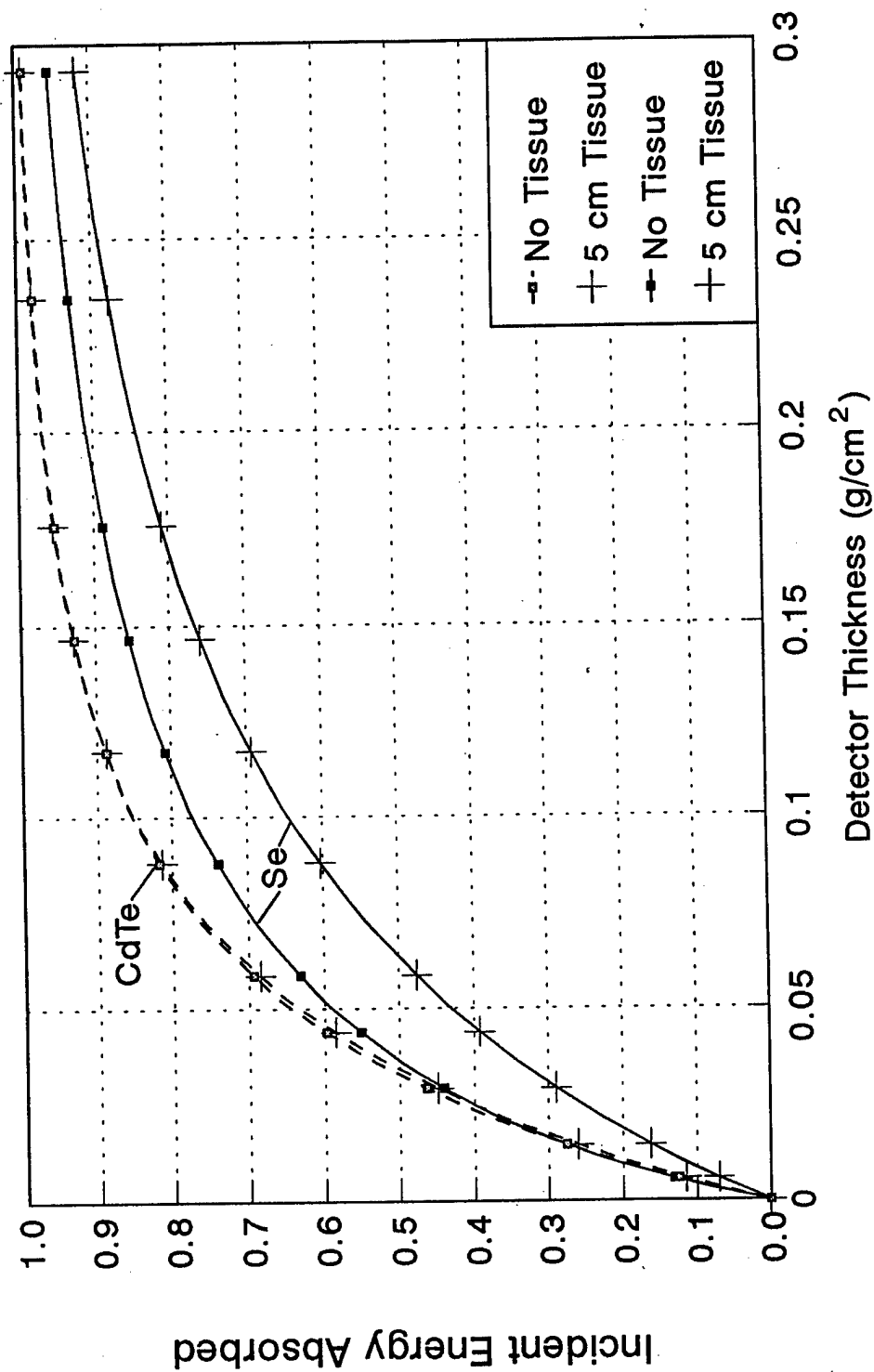
ENERGY DEPOSITION IN CdZnTe AND ZnSe AS A FUNCTION OF THICKNESS
30 kV Molybdenum Spectrum 1.0 mm Be 0.03 mm Mo



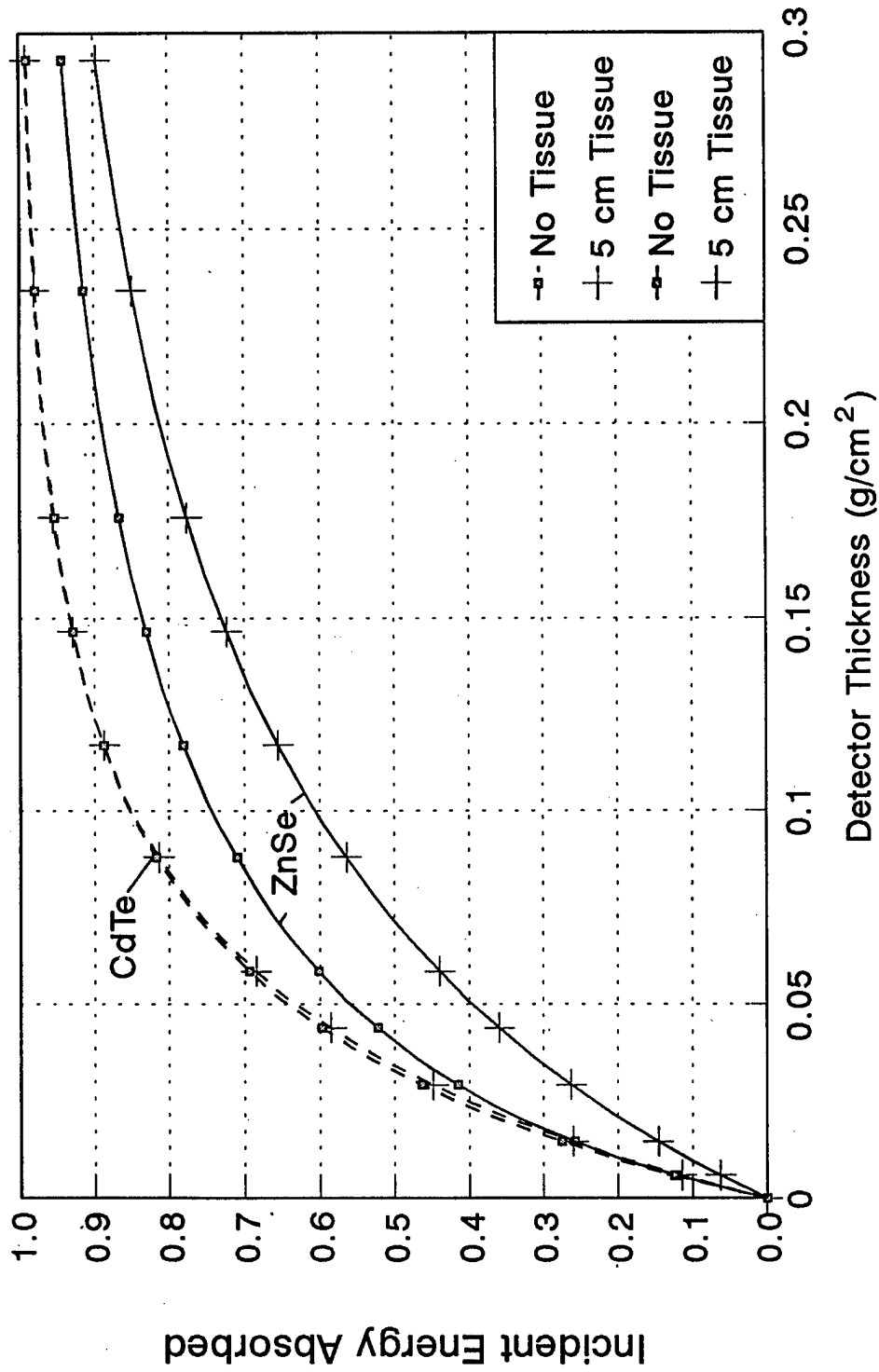
ENERGY DEPOSITION IN CdTe AS A FUNCTION OF THICKNESS
50 kV Tungsten Spectrum 1.0 mm Be 0.5 mm Al



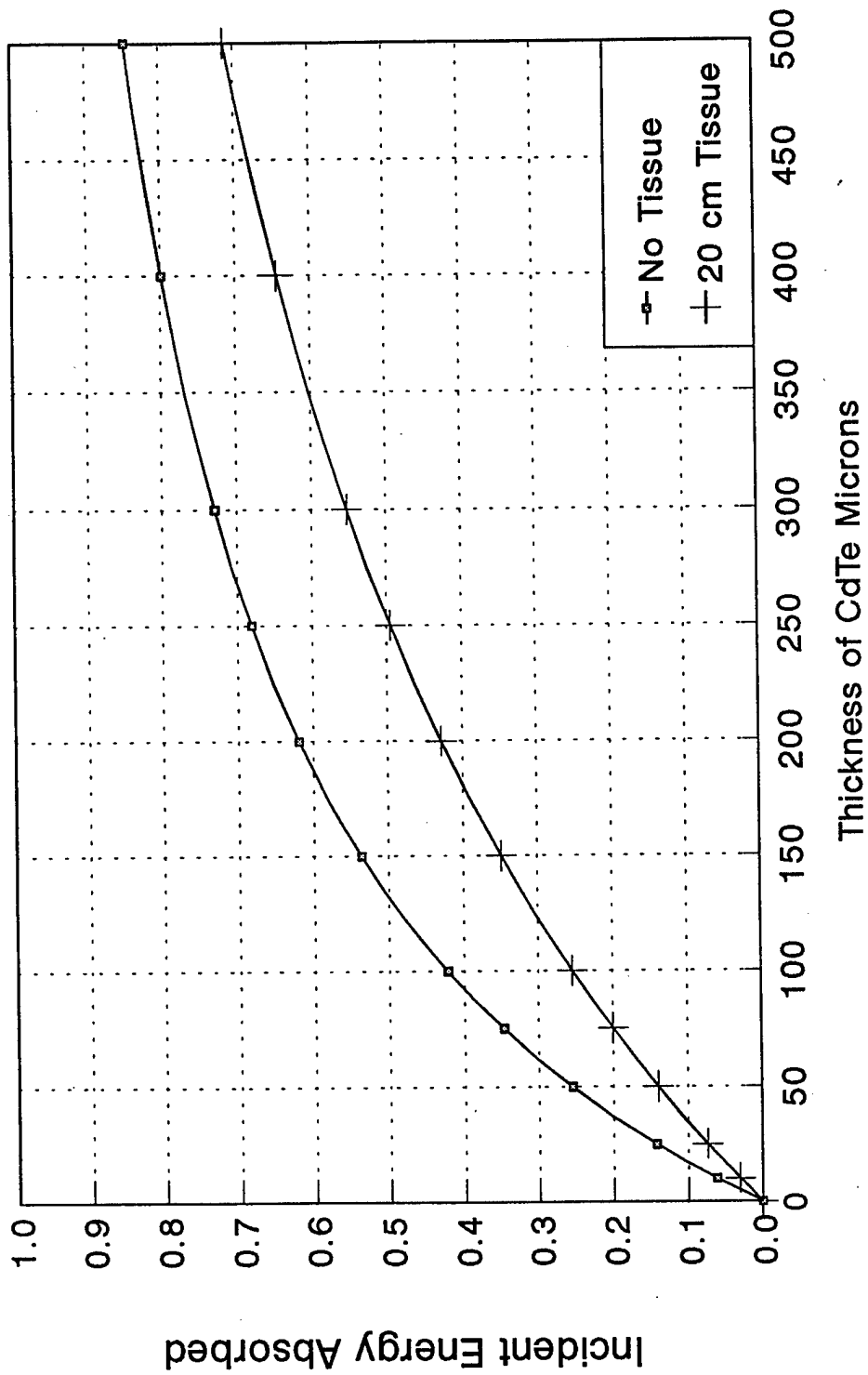
ENERGY DEPOSITION IN CdTe AND Se AS A FUNCTION OF THICKNESS 50 kV Tungsten Spectrum 1.0 mm Be 0.5 mm Al



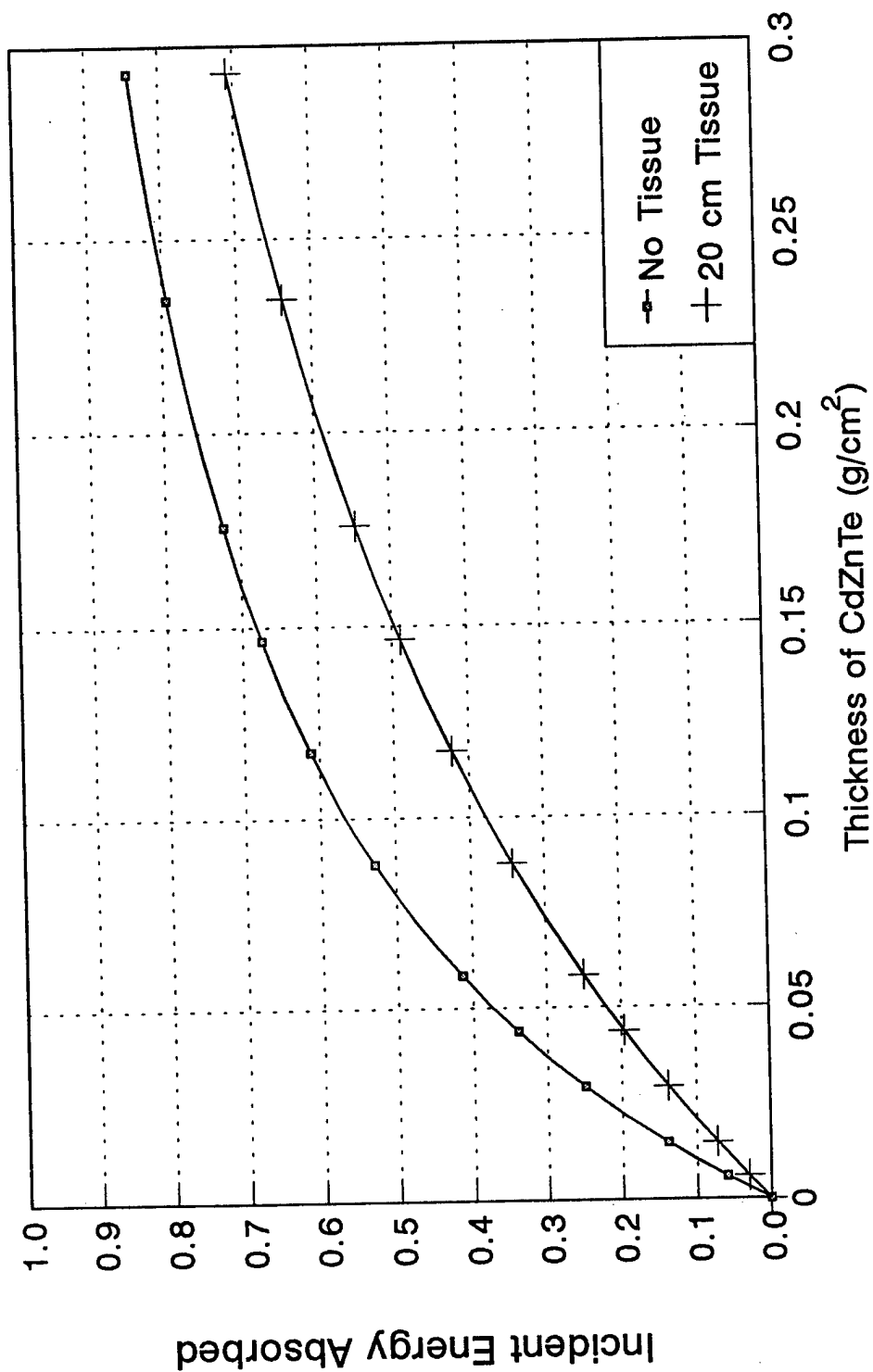
ENERGY DEPOSITION IN CdTe AND ZnSe AS A FUNCTION OF THICKNESS
50 kV Tungsten Spectrum 1.0 mm Be 0.5 mm Al



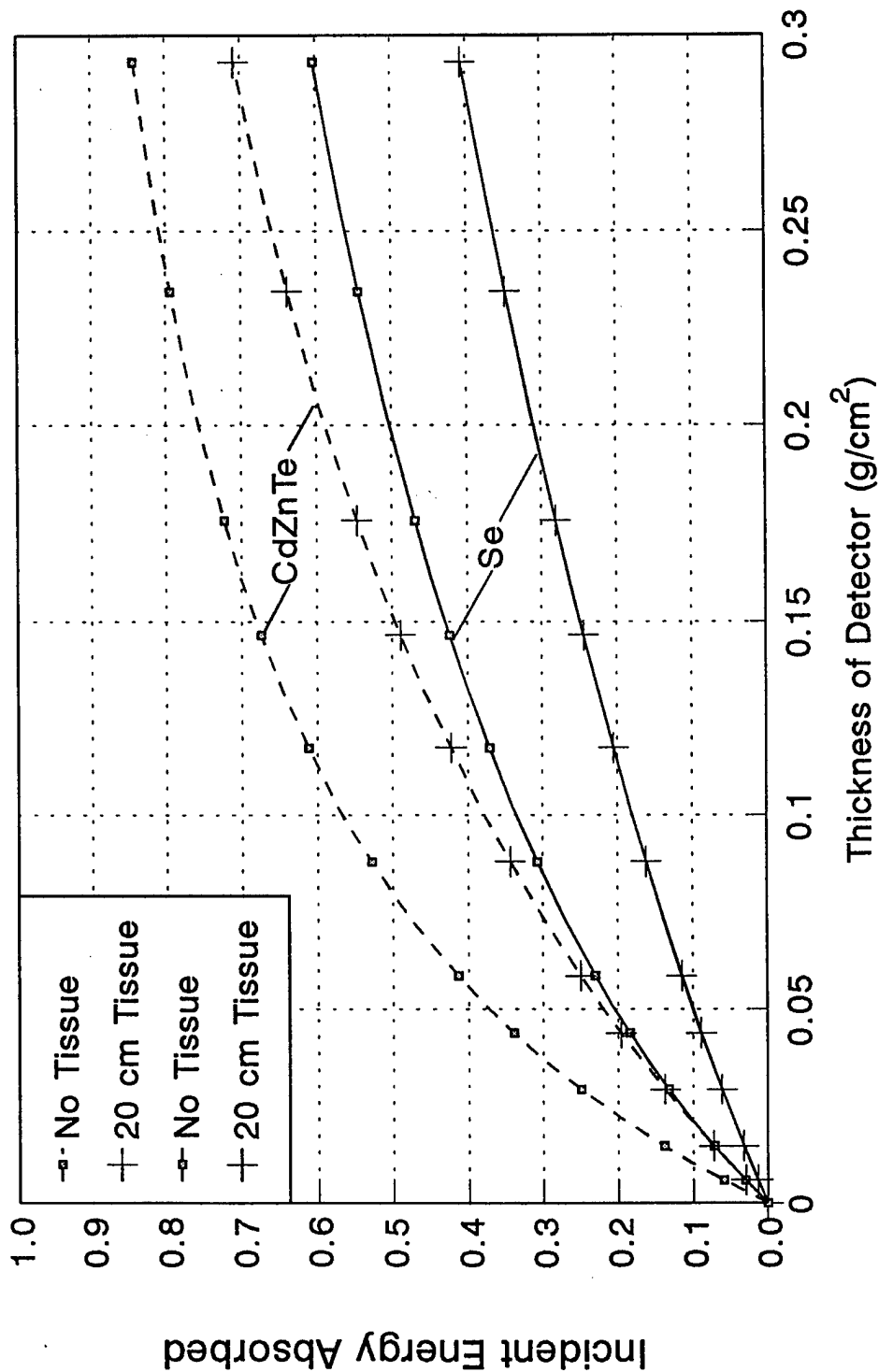
ENERGY DEPOSITION IN CdTe AS A FUNCTION OF THICKNESS
100 kV Tungsten Spectrum 2.5 mm Al



ENERGY DEPOSITION IN CdZnTe AS A FUNCTION OF THICKNESS
100 kV Tungsten Spectrum 2.5 mm Al



ENERGY DEPOSITION IN CdZnTe AND Se AS A FUNCTION OF THICKNESS
100 kV Tungsten Spectrum 2.5 mm Al



ENERGY DEPOSITION IN CdZnTe AND Se AS A FUNCTION OF THICKNESS
100 kV Tungsten Spectrum 2.5 mm Al

